Journal of
Composites Science

MDPI

Review

Bioactive Calcium Phosphate-Based Composites for Bone Regeneration

Marta Tavoni †, Massimiliano Dapporto *,†, Anna Tampieri and Simone Sprio *

Institute of Science and Technology for Ceramics—National Research Council of Italy (ISTEC-CNR), 48018 Faenza, Italy; marta.tavoni@istec.cnr.it (M.T.); anna.tampieri@istec.cnr.it (A.T.)

* Correspondence: massimiliano.dapporto@istec.cnr.it (M.D.); simone.sprio@istec.cnr.it (S.S.); Tel.: +39-0546699760 (M.D.)

† Co-first author, these authors contributed equally to this work.

Abstract: Calcium phosphates (CaPs) are widely accepted biomaterials able to promote the regeneration of bone tissue. However, the regeneration of critical-sized bone defects has been considered challenging, and the development of bioceramics exhibiting enhanced bioactivity, bioresorbability and mechanical performance is highly demanded. In this respect, the tuning of their chemical composition, crystal size and morphology have been the matter of intense research in the last decades, including the preparation of composites. The development of effective bioceramic composite scaffolds relies on effective manufacturing techniques able to control the final multi-scale porosity of the devices, relevant to ensure osteointegration and bio-competent mechanical performance. In this context, the present work provides an overview about the reported strategies to develop and optimize bioceramics, while also highlighting future perspectives in the development of bioactive ceramic composites for bone tissue regeneration.

Keywords: calcium phosphates; hydroxyapatite; scaffolds; bone cements; bioactive composites; bone regeneration

Citation: Tavoni, M.; Dapporto, M.; Tampieri, A.; Sprio, S. Bioactive Calcium Phosphate-Based Composites for Bone Regeneration. *J. Compos. Sci.* **2021**, *5*, 227. https://doi.org/10.3390/jcs5090227

Academic Editor: Francesco Tornabene

Received: 28 July 2021
Accepted: 18 August 2021
Published: 27 August 2021

1. Introduction

Musculoskeletal diseases are a worldwide cause of disability and pain, as they involve bones, teeth and joints, which are anatomical districts relevant for structural support, handling, protection, locomotion, mastication and many other physiological functions [1–3].

Bones are complex structures continuously undergoing dynamic remodeling due to a complex interaction of multiple biochemical processes, primarily ascribable on two different cell lines, osteoblasts and osteoclasts, as actors of bone deposition and resorption, respectively. Such processes can occur spontaneously in the case of minimal bone damage; however, if massive bone defects occur, as a result of a metabolic or traumatic cause, the physiological bone healing process has to be supported by a solid 3D scaffold, acting as a physical and instructive guide for cells [4–8].

Some properties requested for ideal bone scaffolds include *biocompatibility*, which is the ability of a biomaterial to function in vivo without eliciting any adverse side effects; *bioactivity*, which is the additional ability of a biomaterial to chemically bond with the surrounding tissue and to participate in specific biologically relevant phenomena (e.g., ion exchange); and *bioresorbability*, which is the ultimate ability of the implanted material to be resorbed over time, by active participation in physiological turnover reactions, favoring the formation of new tissue [9–12]. More specifically, scaffolds should exhibit *osteoinductivity* and *osteoconductivity*, both stimulating the osteointegration of the scaffold, which consists of a direct bone–scaffold interaction without fibrous tissue at the interface, essential to ensure mechanical stability and also the in-growth of blood vessels. In this respect, a leading concept guiding scaffold development is the achievement of high

mimicry with targeted bony tissues, aiming to achieve a physiological cell response while preventing adverse foreign body reactions [13].

The design and development of biomimetic bone scaffolds have to be inspired by the complex physiological bone composition and structure. The bone microstructure is the result of the biomineralization of type I collagen, secreted by fibroblasts and osteoblasts cells, as a major component of the extracellular matrix of skin, tendon and bone [14]. Osteoblasts create the nano-composite structure of bone by secreting the ions responsible for the formation of apatite crystals. In turn, the ECM influences the adhesion, proliferation and differentiation of osteoblast, osteoclast and osteocyte [5,12]. The ECM is composed of inorganic and organic phases and water: the organic component consists of collagen and non-collagenous proteins, and the inorganic component contains calcium phosphate (mainly plate-like nanocrystalline hydroxyapatite, HA), calcium carbonate, magnesium phosphate and magnesium fluoride doped with various anionic (HPO_4^{2-}, CO_3^{2-} and Cl^-) and cationic species (Na^+, K^+, Mg^{2+}, Sr^{2+}, Zn^{2+}, Ba^{2+}, Cu^{2+}, Al^{3+}, Fe^{2+} and Si^{2+}) trapped in the crystal structure. Carbonate ions are found in extent up to 8 wt%, while Na^+, Mg^{2+}, K^+, Sr^{2+}, Zn^{2+}, Ba^{2+}, Cu^{2+}, Al^{3+}, $Fe^{2+/3+}$, F^-, Cl^- and Si^{4+} ions occur at trace (<1 wt%) [15]. Biogenic HA in bony tissue is non-stoichiometric with a Ca/P ratio between 1.5 and 1.67, where the inclusion of foreign ions in the crystal structure influences solubility, bioactivity, surface chemistry and morphology [16,17]. The general chemical formula for biogenic apatite is $Ca_{10-x}(PO_4)_{6-x}(HPO_4 \text{ or } CO_3)_x(OH \text{ or } \frac{1}{2}\ CO_3)_{2-x}$ with $0 \leq x \leq 2$. One of the most common doping ions in biogenic HA is CO_3^{2-} ions, which can replace both phosphate and hydroxyl ions (leading to type B and type A carbonated apatite, respectively). For example, in B-type carbonated HA, the presence of CO_3^{2-} ions in the phosphate site inhibits the crystal growth and decreases the crystallinity; this structural disorder increases the chemical reactivity and enhances the solubility without changing the affinity of the osteoblast cells. Other possible anionic substitutions are with fluoride and chloride ions [17,18]. Cationic substitutions generally involve monovalent and bivalent cationic in the calcium sites of HA crystal lattice as reported in Table 1 [18–20].

Table 1. Relevant cation substitutions in natural HA crystal structure.

Cations	Biological Effects
Magnesium	Enhancing skeletal metabolism and bone growth
Strontium	Increasing bone mass: stimulating bone formation and reducing bone resorption (anti-osteoporotic agent)
Silicon	Stimulating extracellular matrix formation and mineralization
Zinc	Stimulating osteoblastic activity in vitro and inhibiting bone resorption in vivo

The bone structure exhibits a complex hierarchical architecture resulting from complex interactions of multilevel components, from micrometric osteons to apatite nanocrystals [21] (Table 2).

Table 2. Main components of bone structure, from macroscale to nanoscale.

Macrostructure	Cortical bone Spongy bone
Microstructure	Osteons (100 μm) Haversian canals (10 μm) Collagen fibrils (25–500 nm)
Nanostructure	Tropocollagen triple helix Collagen molecule Hydroxyapatite nanocrystals (30 nm)

In particular, it is possible to classify the levels and structures of components as follows:

1. Macrostructure: cancellous and cortical bone;
2. Microstructure: (10–500 mm): Haversian channel, osteons and single trabeculae;
3. Sub-microstructure (1–10 mm): lamellae;
4. Nanostructure (100 nm–1 mm): fibrillar collagen and embedded mineral;
5. Sub-nanostructures (<100 nm): molecular structure of constituent elements, such as minerals, collagen and non-collagenous proteins [22].

Such a complexity is the main responsible factor for the outstanding mechanical performance of bone and its self-repair ability [23].

The ideal bone scaffolds should be endowed by several physico-chemical features, including chemical composition mimicking both the natural bone ECM and mineral phase, open and interconnected porosity capable of promoting neo-vascularization, tissue ingrowth, nutrient and oxygen supply, nano-structured surface topography positively driving adhesion, proliferation and differentiation of cells, that are adequate mechanical properties able to sustain the biomechanical loads toward the effective regeneration of the tissue.

Several studies have been carried out on the research of biomaterials, such as metals, natural or synthetic polymers, ceramics and composites, which can match all these characteristics, but no one fully satisfies all these requirements [24–30]. In particular, bioceramic-based scaffolds are widely used in numerous biomedical applications, including maxillofacial reconstruction, the stabilization of jaw bones, periodontal disease, as space fillers, self-hardening bone pastes/cements and as a coating on implants, due to their positive interaction with human tissue. Bioceramic-based materials can be classified as bioactive and bioinert materials. Ceramics considered as bioinert include alumina and zirconia; they show high chemical stability in vivo as well as high mechanical strength. However, they do not have osteogenic properties [31]. Bioactive ceramics, such as calcium phosphates (CaPs), silicates, bioactive glass, and titanium oxide, are capable of interacting with cells and thus able to promote and stimulate bone regeneration [28–33].

CaP bioceramics are widely used as bone substitutes since the 1920s and are considered as the golden standard in bone regeneration due to their similarity to the inorganic bone [34–37]. The chemical composition of CaPs relies on multiple ions, including calcium (Ca^{2+}), orthophosphate ($PO_4{}^{3-}$), metaphosphate ($PO_3{}^{-}$), pyrophosphate ($P_2O_7{}^{4-}$) and hydroxide (OH^{-}) [9,37] (Table 3).

Table 3. Some CaP materials: name, abbreviation, chemical formula, Ca/P ratio and solubility.

Name	Abbreviation	Chemical Formula	Ca/P Ratio	Solubility at 25 °C, mg/L
Hydroxyapatite	HA	$Ca_{10}(PO_4)_6(OH)_2$	1.67	~0.3
Calcium-deficient hydroxyapatite	CDHA	$Ca_{10-x}(PO_4)_{6-x}(HPO_4$ or $CO_3)_x(OH$ or $\frac{1}{2}$ $CO_3)_{2-x}$	1.5–1.67	~9.4
Dicalcium phosphate dihydrate	DCPD	$CaHPO_4{\cdot}2H_2O$	1	~88
α-Tricalcium phosphate	α-TCP	α-$Ca_3(PO_4)_2$	1.5	~2.5
β-Tricalcium phosphate	β-TCP	β-$Ca_3(PO_4)_2$	1.5	~0.5

The solubility of CaP compounds strongly influences their behavior in vivo [37].

Among CaPs, HA is particularly promising for bone tissue regeneration due to its very close composition with natural apatite. In the last decades, the synthesis of HA has been investigated for different applications, including scaffolds, injectable pastes/cements, coatings for metallic implants and in nanomedicine as drug delivery platforms [38,39].

HA can be produced by several methods: high-temperature solid-state reactions or low-temperature precipitation [38]. Stoichiometric HA exhibits high stability at physiological pH, limiting its long-term resorption. Therefore, various recent studies have been focused on increasing the solubility and osteogenic activity of HA by ionic doping [39,40].

The notable interest in TCP comes from the combination of its solubility and low Ca/P ratio, particularly interesting when obtaining apatite crystals in an aqueous environment [16].

There are two polymorphs of TCP: the high-temperature α-TCP and the low-temperature β-TCP[41]. The β-TCP polymorph is stable at room temperature, while a transformation into α-TCP occurs at temperatures higher than 1125 °C. Besides a similar chemical composition, the TCP polymorphs have different crystalline structures, density and solubility, thus also resulting in different biological performance. The α-TCP phase is more soluble than β-TCP and can be easily hydrolyzed in calcium-deficient hydroxyapatite (1).

$$3\ Ca_3\ (PO_4)_2 + H_2O \rightarrow Ca_9(HPO_4)(PO_4)_5OH \quad (1)$$

In addition, several ions can be introduced in the structure of TCP (Mg^{2+}, Sr^{2+}, Zn^{2+}, Si^{2+}, etc.), opening different thermodynamic scenarios in terms of polymorph stabilization; e.g., silicon was reported to stabilize α-TCP, while magnesium ions stabilize β-TCP.

Due to its high solubility, TCP has been used for the preparation of biphasic CaP scaffolds, able to conjugate the osteogenic properties of HA and the resorption behavior of TCP [42,43].

DCPD is biocompatible, biodegradable and osteoconductive [9]. DCPD can be prepared by the neutralization of phosphoric acid with calcium hydroxide at pH 3–4 at room temperature. DCPD can be obtained by double decomposition between calcium- and phosphate-containing solutions in slightly acidic media. It can also be formed by the conversion of calcium phosphate salts, in acidic media, or by the reaction of calcium salts, such as calcium carbonate in acidic orthophosphate solutions. In vivo studies showed that DCPD converts into HA or it degrades and is replaced by bone [44–46]. Brushite, in medicine, is used in CaP paste/cement and as an intermediate for tooth remineralization [44,47].

Other silica-based bioceramics have also been studied as bone scaffolds, including wollastonite ($CaSiO_3$), larnite (Ca_2SiO_4), hatrurite (Ca_3SiO_5), monticellite ($CaMgSiO_4$), diopside ($CaMgSi_2O_6$), akermanite ($Ca_2MgSi_2O_7$), merwinite ($Ca_3MgSi_2O_8$), silicocarnotite ($Ca_5(PO_4)_2SiO_4$), nagelschmidtite ($Ca_7(SiO_4)_3(PO_4)$) and bioglass [48]. Silicon ions participate in bone metabolism, and silica-based materials exhibit good biological response in vitro, resulting in bioactive, biocompatible, bioresorbable, osteoinductive and osteoconductive behavior. The favored formation of apatite in physiological fluid was reported, thus facilitating the chemical interaction into the living bone structure following implantation [29,32].

The following steps explain the formation of apatite on the surface of silica-based bioceramics:

- The rapid exchange of Ca^{2+} with H^+ or H_3O^+ from a body fluid solution results in the hydrolysis of silica groups, which creates silanol, according to Si-O-Ca^+ +H^+→ Si-OH^+Ca^{2+}(aq).
- The loss of soluble silica in the form of $Si(OH)_4$ to the body fluid, resulting from the breaking of Si-O-Si bonds and the formation of silanol (Si-OH) at the glass solution interface: Si-O-Si + H_2O → 2Si-OH.
- The condensation and polymerization of a SiO_2-rich layer on the surface short in alkalis and alkaline earth cations: Si-OH+HO-Si → Si-O-Si+H_2O.
- The migration of $Ca_2{}^+$ and $PO_4{}^{3-}$ groups to the surface via the SiO_2-rich layer forming a CaO-P_2O_5-rich film by the incorporation of soluble calcium and phosphates from the solution.
- The crystallization of the amorphous CaO-P_2O_5-rich film by the addition of OH^- and $CO_3{}^{2-}$ anions from body fluid forms a mixed hydroxyl, carbonated apatite layer.
- The adsorption and desorption of biological growth factors on the carbonated apatite layer to activate stem cells.
- The action of macrophages to remove debris from the site allowing cells to occupy their space.
- The attachment of stem cells to the bioactive surface and its differentiation to form osteoblasts.

- The generation of ECM by the osteoblast to form new bone and its crystallization in the living composite structure.

Bioglasses are also a class of bioactive, osteoconductive and osteoinductive materials essentially composed of silicate, calcium, sodium and phosphate (e.g., composition of Bioglass 45S5® (wt%) 45 SiO_2, 24.5 CaO, 24.5 Na_2O, 6 P_2O_5). Upon implantation, bioglasses are not surrounded by fibrous tissue but form a strong, integrated bond to bone. In fact, when immersed in body fluids, the formation of a silica-rich layer on its surface takes place, which converts to a silica-CaO/P_2O_5-rich gel layer as a precursor of HA layer formation [24,33]. In addition, they are able to release ions, which enhance gene up-regulation and favor bio-degradation, in turn favoring bone regeneration [49]. Major drawbacks are related to the difficult consolidation of bioglasses into 3D porous scaffolds, as the required thermal treatment easily provokes the crystallization of oxides, thus losing the bioactive properties related to the material in its amorphous state. Therefore, alternative consolidation methods are currently under investigation; however, a major issue remains regarding the achievement of substantial mechanical properties associated with open porosity [50].

The mechanical properties of scaffolds play an important role in bone tissue engineering. The relevant mechanical properties of bone include Young's modulus, toughness, shear modulus, tensile strength, fatigue and compressive strength. Several approaches have been reported to increase the mechanical performance and load transfer efficiency between the scaffold and the surrounding bone tissue, mainly related to stronger interfacial bonding of the coating layer to the substrate [51].

The mechanical strength of ceramics mainly relies on their chemical composition, grain size, porosity extent and internal structural defects [37] (Table 4).

Table 4. Ideal features of scaffolds for bone regeneration, with respective proposed strategies to improve them.

Properties	Proposed Improving Strategies
Open and interconnected porosity	• Traditional techniques for the fabrication of a 3D porous device (sacrificial template, direct foaming) • Low-temperature self-hardening methods • Biomimetic and biomorphic synthesis • 3D printing technology
Mechanical properties	• Reinforced scaffold by compression, using fibers (polymeric or ceramic) or a dual setting system
Biofunctionality	• Biomimetic and biomorphic synthesis • Surface topography modifications
Bioactivity	• Biomimetic and biomorphic synthesis • Ion-doping ceramic-based scaffold • Ceramic-based composites

Bioceramics typically exhibit higher compressive than tensile strength, but they are also intrinsically brittle, leading to sudden failure during handling and fixation [52]. In this respect, a critical challenge is related to the optimization of toughening mechanisms for ceramics [53,54].

The enhancement of the performance of bioceramic scaffolds has been widely explored by the combination of different calcium phosphate phases into bioceramic composites. The present work aims to provide the reader with an overview about the recently reported strategies to enhance the biofunctionality and mechanical properties of bioceramic scaffolds. In particular, various manufacturing techniques are explored, including the replica method, the sacrificial template, direct foaming, the low-temperature self-hardening method and biomorphic and biomimetic synthesis, as well as 3D printing, while also highlighting

future perspectives for the development of bioactive ceramic composites and devices with enhanced biofunctional properties (Figure 1).

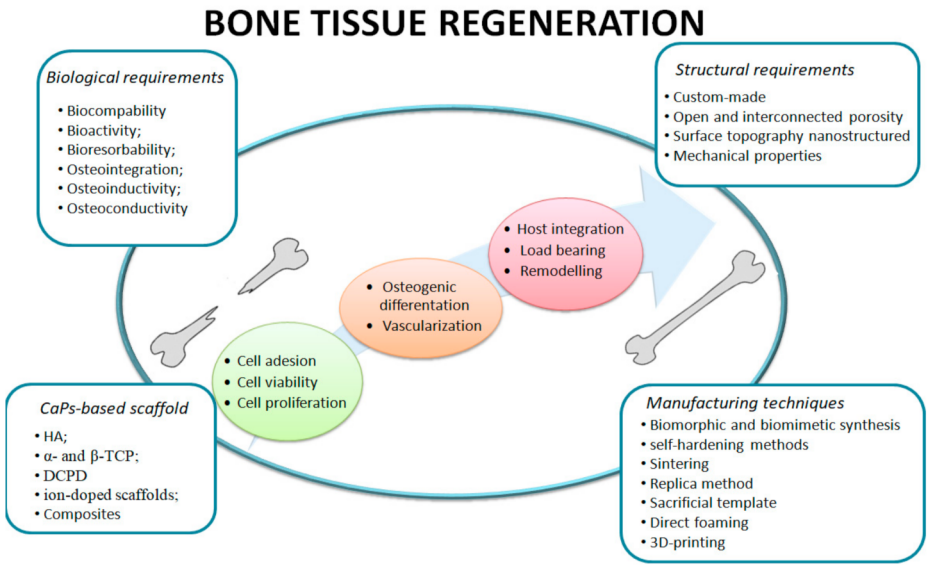

Figure 1. Flow chart of biological and structural requirements underlying the ideal scaffold for bone tissue regeneration.

2. Fabrication of Bioceramic Composites

The biological events occurring upon implantation of a scaffold for bone regeneration are strongly influenced by pore size distribution. The scaffold porosity affects the capability of the surrounding tissue to promote cell infiltration, migration, vascularization and nutrient and oxygen flows [18,55]. The morphological properties of scaffolds in terms of pore volume and size are important at both the macroscopic and the microscopic level.

It was reported that osteointegration and angiogenesis can be favored by interconnected macroporosity (100–600 μm) with channel-like microporosity [18]. A pore size increase is generally associated with an increase in permeability and the new bone ingrowth, while small pores are more suitable for soft tissue in-growth.

Over the past two decades, several technologies have been developed for the manufacturing of highly porous bioceramic-based scaffold for bone tissue regeneration [15,17,31,40–47]. In the next paragraphs, we explore the main fabrication techniques of porous scaffolds: traditional methods (partial sintering, replica method, sacrificial template and direct foaming), low-temperature self-hardening methods, biomorphic and biomimetic synthesis and 3D printing technology.

2.1. Macroporous Compositescaffolds

The development of materials with tailored porosity has been a matter of intense research in the last decades, particularly in the case of composite scaffolds for bone tissue regeneration, because of the crucial role of voids in the structure to guide and facilitate cell proliferation and neovascularization [56].

One of the first reported approaches to tune the porosity of ceramics was the partial sintering process: the pore size distribution is mainly affected by powder particle size and sintering temperature, as higher sintering temperatures induce a significant decrease in intergranular porosity [57,58].

A great research effort has also been devoted to the preparation of macroporous bioceramic scaffolds, leading to the establishment of various techniques, including template-assisted (replica and sacrificial template) and template-free techniques (direct foaming) [56,59,60] (Table 5) [56,60].

Table 5. Main processing steps involved in the fabrication of porous bioceramics.

Template-Assisted Techniques	Processing
Replica	• Preparation of stable ceramic suspension • Impregnation of synthetic/natural porous template into the ceramic suspension • Drying and template removal • Sintering
Sacrificial template	• Preparation of ceramic or ceramic precursor in solid or liquid form • Addition of sacrificial phase • Drying, pyrolysis and evaporation • Sintering
Template-Free Technique	
Direct foaming	• Preparation of stable ceramic suspension • Addition of surfactants • Incorporation of gas • Drying of the foamed suspension • Sintering

These methods generally involve the preparation of slurries, intended as aqueous suspensions of dispersed powders; then, the slurries are properly manipulated, dried and thermally consolidated.

The replica method is a template-assisted technique based on the impregnation of a polymeric sponge with a defined porous structure and pore size into the ceramic slurry in order to produce microporous structures exhibiting the original sponge morphology [56]. The templates used in this technique can be either synthetic or natural polymers (e.g., polyurethane and cellulose, respectively). The macroporous scaffolds obtained with this method can reach an anisotropic porosity ranging from 40 to 95% and are characterized by a cross-linked structure with highly interconnected pores ranging in size from 200 μm to 3 mm [56].

The sacrificial template method involves the homogeneous dispersion of sacrificial phases into a continuous matrix of ceramic particles or ceramic precursors, followed by drying and sintering. A wide variety of sacrificial materials can be used as pore-forming agents, including natural polymers (e.g., gelatin, potato starch, cotton), synthetic polymers (e.g., polymer beads, organic fibers, polyethylene) and inorganic polymers (e.g., NaCl, K_2SO_4). The removal of sacrificial materials from the matrix can be achieved by thermal treatments or chemical processes. This method leads to porosity ranging from 20 to 90%, with an average pore diameter of 1–700 μm [18,56].

Template-free foaming techniques are particularly promising due to the absence of massive amounts of organic phases to be eliminated during thermal consolidation. Direct foaming represents an easy, cheap and fast way to prepare macroporous bioceramics with open porosity from 40 to 97% and pore size 10 μm–1 mm by incorporating gas bubbles into ceramic slurries, followed by drying and sintering [18,56,61]. The total porosity volume is related to the amount of gas bubbles incorporated during the foaming process, whereas the pore size depends on the stability of the poured foam before drying [18,56,61].

The sacrificial template approach also includes the freeze-casting method, which is based on the controlled freezing of liquid-based ceramic slurries [18]. The freezing of the liquid, generally water, induces the formation of anisotropic ice structures, intended as fugitive materials, during the subsequent freeze-drying process [62]. The efficacy of the process is affected by several parameters, including the viscosity of the slurry, the solvent and the freezing control in space and time. Typical structures obtained by freeze-casting methods showed well-defined pore connectivity along with directional and completely open porosity, such as a lamellar morphology after sintering [63]. The channel-

like anisotropic porosity obtained by the freeze-casting method may lead to scaffolds with channels similar to cortical bone, particularly useful for long bone applications [18].

2.2. Self-Hardening Bioceramic Composites

The possibility to obtain bioactive ceramics through low-temperature self-hardening processes has been widely explored in the form of bone cements for injectable orthopedic applications, including spinal fusion, vertebroplasty and kyphoplasty [30,64–66]. Bone cements refer to pastes able to self-harden under physiological conditions and can be injected in vivo through minimally invasive surgery [64]. The first bone cement used in orthopedics was based on polymers, in particular polymethylmethacrylate (PMMA) in 1958, and, in the 1970s, the FDA approved bone cement for use in hip and knee prosthetic fixation [67]. Despite PMMA-based cements exhibiting good handling, setting times and mechanical performance, they are not osteogenic nor bioresorbable. Calcium phosphate cements (CPC) were discovered by Brown and Chow in the 1980s [68–70], overcoming the drawbacks of PMMA cements in terms of exothermic polymerization hardening and chemical composition. In this respect, CPCs exhibit bioactivity, bioresorbability and a physiological hardening at 37 °C, also allowing the incorporation of biomolecules [68]. The main drawback of CPCs hampering their clinical applications is related to their poor mechanical performance, which limits their applicability to a moderate- or non-load-bearing situation [71].

CPCs can be classified by several parameters, including the number of components in the solid phase, the type of setting reaction and the type of end product (Table 6) [38,68].

Table 6. Classification of CPC.

	Apatitic CPC		**Brushitic CPC**
	Single Component	**Multiple Components**	
Reactives	α-TCP	TTCP + DCPA/DCPD	B-TCP + MCPM/MCPA
Reaction type	Hydrolysis		Acid-Base
Reaction	$3\alpha - Ca_3(PO_4)_2 + H_2O \rightarrow Ca_9(HPO_4)(PO_4)_5(OH)$	$Ca_4(PO_4)_2O + 2CaHPO_4 \rightarrow Ca_{10}(PO_4)_6(OH)$	$\beta - Ca_3(PO_4)_2 + Ca(H_2PO_4)_2 \cdot H_2O + 7H_2O \rightarrow 4CaHPO_4 \cdot 2H_2O$

Many different formulations of CPCs have been developed, and they can be divided into two groups based on the type of end product: brushite (DCPD) and apatite (HA or CDHA) cements. Both brushite and apatite CPCs are produced upon mixing one or more CaP powders with aqueous solutions, which induces the dissolution of the initial CaPs; this is followed by precipitation into crystals of DCPD, HA or CDHA depending on the compositions of the powders and the setting reactions that take place [38,72]. During precipitation, new apatitic crystals grow and their physical entanglement causes the hardening or setting at body temperature.

Apatitic CPCs can be obtained by mixing single or multi-components with aqueous solutions that undergo hydrolysis or acid–base reactions, respectively. In the first case, the end product is calcium-deficient hydroxyapatite (CDHA), and in the latter, it is stoichiometric HA [64,68]. Some examples are as follows:

- Hydrolysis of metastable α-TCP:

$$3\ \alpha\text{-}Ca_3(PO_4)_2 + H_2O \rightarrow Ca_9(HPO_4)(PO_4)_5(OH)$$

- Acid–base reaction between tetra calcium phosphate, TTCP (basic), and di calcium phosphate anhydrous, DCPA (acidic):

$$Ca_4(PO_4)_2O + CaHPO_4 \rightarrow Ca_5(PO_4)_3(OH)$$

Brushite CPC obtained by an acid–base reaction between TCP (almost neutral) and monocalcium phosphate monohydrate, MCPM (acidic):

$$\beta\text{-}Ca_3(PO_4)_2 + Ca(H_2PO_4)_2 \cdot H_2O + 7H_2O \rightarrow 4\ CaHPO_4 \cdot 2H_2O$$

Two of the most important parameters that play a key role in the final CPC features are the liquid-to-powder ratio (LPR) and the particle size of the starting powder [37,68]. The LPR influences setting time, injectability, cohesion, mechanical properties and the porosity of harder CPC [73]. The setting time is the "time required from the start of powdered agent and liquid agent blending until hardening of the cement", according to ISO/DIS 18531 for CaPs [30,74], and influences the clinical applicability of both apatite and brushite cements as well as their injectability [30,74].

Both particle size and the LPR influence the final surface morphology of the brushite or apatite crystals and the total porosity of the final scaffolds, which affects the mechanical performance and the resorbability of scaffolds and therefore the overall bioactivity (Table 7) [37,68]. The reduction in the particle size of CaPs increases the surface area, thus affecting the reaction kinetics and yielding small needle-like crystals rather than large plate-like crystals as observed when larger CaP precursor particles are used [38,75]. Moreover, porosity is also attributed to the amount of liquid phase used; thus, by increasing the LPR, the amount of liquid phase decreases, and the porosity increases. This effect of the LPR explains the difference between brushite and apatite cement in terms of microstructure porosity: the water consumption during the setting reaction of brushite cement is larger than that of the apatite, which leads to the formation of a larger crystal size and makes the total porosity smaller and average pore size greater than those of the apatitic cements [37,73]. The typical porosity of CPC ranges between nano- and sub-micrometer size, allowing the flow of physiological fluids within the microstructure of the cement, but the pores are too small to facilitate the growth of bone tissue; in this regard, porogens are often used [69].

Table 7. Effect of particle size and liquid-to-powder ratio on the crystals' morphology and pore distribution.

	Particle Size		**Liquid-to-Powder Ratio**	
	Fine Particles	**Coarse Particles**	**Low L/P**	**High L/P**
Final crystal morphology	Needle-like crystals	Plate-like crystals	Low inter-aggregate distance	High inter-aggregate distance
Pore size distribution	Fine	Coarse	Fine	Coarse

As mentioned above, increasing porosity leads to decreasing mechanical strength; thus, a compromise must be sought between mechanical performance and porosity degree.

One of the advantages of CPC is the room-temperature self-hardening mechanism, which, combined with the intrinsic porosity, allows the incorporation of drugs, biologically active molecules and cells, obtaining drug delivery materials [76,77]. The incorporation of active molecules in CPCs can be achieved by dissolving it in the liquid phase or by a combination with the powder phase of the CPC mixing setting [68,78]. Another possible approach is the superficial adsorption of drugs on the CPC surface by incubation of the scaffold in the drug solution: the kinetic release of drugs depends on the functionalization, microstructure and resorbability of the CPC matrix [68,78].

2.3. Biomorphic Transformations

A valuable approach to obtain bioceramic composite scaffolds with a complex structural hierarchy relies on biomorphic transformations of natural structures mimicking the morphology and microstructure of the target tissue [20,77,79].

Since the 1970s, biomorphic transformations from natural sources have been proposed for the fabrication of bioceramic scaffolds due to their 3D highly interconnected porous architecture, including the replica of the porous microstructure of $CaCO_3$-based corals,

which are impossible to create artificially, and the replica of marine sponges, soft vegetal structures and fruit- and wood-template bioceramics [75,80,81].

The approach of wood biotransformation is particularly interesting, as many ligneous species exhibit a porous and hierarchically organized structure very close to that of cortical and cancellous bone. The transformation of wood generally involves pyrolysis followed by a hydrothermal treatment; in particular, a complex multi-step strategy to convert rattan wood structures into biomimetic HA scaffolds was proposed [76,77,82]. In particular, several subsequent and strictly controlled reactions are required, including (i) the *pyrolysis* of wood to produce a carbon template; (ii) *carburization*, calcium infiltration to transform carbon in CaC_2; (iii) an *oxidation* process that leads to CaO formation; (iv) *carbonation* by hydrothermal processes or by heterogeneous processes carried out at supercritical conditions and high pressure; and finally (v) *phosphorylation* through the hydrothermal process generating biomimetic, hierarchically organized scaffolds made of ion-doped HA.

2.4. 3D Printing

Three-dimensional (3D) printing represents an additive manufacturing (AM) technique (also known as rapid prototyping) to produce complex-shaped devices with complex geometry and design flexibility from 3D model schemes [83–86]. A wide range of materials have been employed with 3D printing techniques, including metals, polymers, ceramics and composites [85,86].

Different 3D printing methods have been proposed [85,87–90]. Extrusion-based techniques consist of the deposition of ink to create designed structures by forcing the ink through a nozzle as a melt, in fused deposition modeling (FDM), or viscous suspensions, in direct ink writing (DIW), to form lines that solidify onto a build plate [90].

DIW represents an easy manufacturing technique that allows the creation of a wide range of structures, from solid monolithic parts to highly complex porous scaffolds and composite materials. The use of pastes also allows shape retention due to the high solid loading and visco-elastic properties. The use of high viscous inks requires larger diameter nozzles compared to the conventional inkjet printing ink; it can therefore be used successfully to print extremely viscous pastes that are HA based [88].

Three-dimensional printing technology finds a wide range of biomedical applications: craniofacial implants, dental models, prosthetic parts, scaffold for tissue regenerations (bone and skin), organ printing, tumor therapy and tissue modeling for drug discovery [90–92]. In these kinds of applications, printable materials are formulated from biomaterials and bio-inspired materials to achieve patient-specific scaffolds with high structural complexity [93]. Moreover, printable biomaterials should be biocompatible and bioactive and should have good degradation kinetics, appropriate mechanical properties, give desirable cellular responses and exhibit tissue biomimicry [94,95].

Bioceramic powders, natural or synthetic hydrogels, polymers and their composites have been used as raw materials to formulate inks for 3D printing; in this review, we focused on ceramic-based scaffolds and bioceramic/polymer composites. Bioceramics commonly printed are calcium phosphate-based bioceramics (HA, TCP and biphasic CaP), calcium silicate-based bioceramics and bioactive glasses [91,93].

Moreover, the precise tuning of the macro- and micro-porosity permitted by 3D printing technology not only allows the fabrication of scaffolds with hierarchical porosity but also leads to the controlled release of biomolecules or drug loaded in the scaffold matrix or adsorbed on the scaffold surface [96,97].

Three-dimensional-printed bioceramics include sintered 3D-printed bioceramics, non-*sintered 3D-printed bioceramics* and *composites with polymers*.In the first case, bioceramic scaffolds are printed and sintered, removing the organic phases and improving the mechanical properties of the structure [93]. In the presence of biologically active ions, such as magnesium or strontium, in addition to an improvement of mechanical properties, an increase in biological performance in vivo was also reported [98]. Another study described biphasic CaP scaffolds (HA:β-TCP with a weight ratio 60:40) coated with calcium perox-

ide and polycaprolactone in order to promote bone growth with greater proliferation of osteoblasts under hypoxic conditions, following the release of oxygen dependent on the concentration of calcium peroxide in the PCL coating [99].

In non-sintered 3D-printed bioceramics, a small amount of organic solvent is used as a binder for bioceramic powders and is not removed after printing. Sun et al. developed a porous 3D scaffold of biodegradable CaP loaded with antibiotics for the regeneration of the bone tissue of the jaw, achieving a controlled drug release. This scaffold was based on an HA or biphasic mixture of CaP (β-TCP and HA with a weight ratio of 1:1) cross-linked with sodium alginate in the presence of the drug, and the paste was then extruded by the 3D printer. By modulating the degree and the time of cross-linking, it is possible to control the drug release kinetics. In vitro studies show low cytotoxicity and good cell adhesion and proliferation on the scaffold surface [100].

Bioceramic and polymer composite are synthesized to combine the bioactivity and osteoconductivity of bioceramics with the handling performance of polymers [87]. For example, the presence of strontium-doped HA nanoparticles in 3D-printed PCL scaffolds leads to a significant increase in cell proliferation and bone regeneration, due to the simultaneous release of calcium and strontium ions, associated with an improvement in mechanical properties as related to the inorganic phase content [101]. HA nanoparticles were also used as an external coating for 3D-printed polymer scaffolds in order to enhance cell proliferation and differentiation while also strengthening the scaffold [94].

Recently, 4D printing approaches have been developed, which, in addition to three-dimensional spatial control, introduces the concept of temporal control, i.e., active smart materials responsive and mechanically converted into other shapes via external stimuli. This technique enables the production of smart 3D scaffolds responding to external stimuli, such as changes in pH and temperature or when subjected to magnetism or light radiation of adequate energy [95,102,103].

3. Enhancing the Biological Performance of Bioceramic Composites

3.1. Biofunctionalization

Biofunctionalization is the modification of a material to achieve improved biological function and/or stimulus, whether permanent or temporary. The biofunctionality of scaffolds for regenerative medicine has been considered to play a key role for effective tissue regeneration [92,95].

Several parameters can be tuned, including surface energy and roughness, Ca/P ratio, solubility, particle size and crystallinity, in order to improve the biological events beyond the interaction with the biological environment, e.g., protein adsorption, cell attachment, cell proliferation and cell differentiation [93,104] (Figure 2).

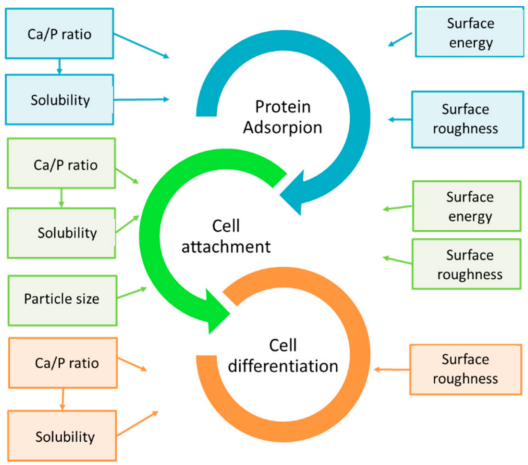

Figure 2. Key properties of CaP-based bioceramics that have an impact on biological events.

The architecture of biomimetic scaffolds greatly affects the chance to obtain a suitable microenvironment for bone regeneration. The presence of a diffuse macroporosity favors cell adhesion, cell proliferation and vascular growth. In turn, the surface micro-architecture enhances protein adsorption, and specific nano-topography could directly modulate the osteogenic differentiation, producing a favorable osteoimmune microenvironment [97]. Among the various microstructures, microgrooves have strong effects in the regulation of cell orientation and adhesion [96,105]. The width of the micro-channels controls the orientation, while the depth regulates the adhesion strength of the cells, which decreases as the depth of the groove increases. Micro–nano hybrid structures (micropattern–nanorod hybrid structure) showed higher cell adhesion, proliferation and ALP (alkaline phosphatase protein) activity than a single-scale structure (including nanorods and micropatterns) [96,106].

The roughness of the surface plays a crucial role in cellular behavior [107–109] (Table 8).

Table 8. Effects of structural size, morphology and roughness surface of CaP biomaterials on cellular behavior.

Surface Structure	Parameters (Size, Morphology, Roughness)	Biological Function	
		Enhance	Decrease
Micro/nano size (CaP)	Microgroove width: From 20–40 um to 60–100 um	Cell number inside the pattern	Cell alignment/orientation
	Microgroove depth From 3 um to 5.5 um		Cell adhesion force
	Microgroove depth pattern: From nano-hybrid to micro-hybrid	Cell adhesion, proliferation, osteogenesis	
Micro-/nano-morphology (CaP)	Micro-morphology: Plate-like and net-like	Cell attachment expansion	
	Nano-morphology: Plate-like and wire-like	Osteogenesis	
Micro-/nano-roughness (CaP)	Micro-roughness: Ra from 1 um to 2 um	Cell attachment osteogenesis	
	Nano-roughness: Ra from 5.3 nm to 9.8 nm	Focal adhesion osteogenesis	

It was demonstrated that specifically designed roughness can enhance osteogenesis due to the modulated concentration of calcium ions and osteocalcin in the grooves [110].

The surface chemistry also plays a key role in cell behavior. The crystallinity of nanometric bioceramics, i.e., ACP and HA, was observed to affect cell attachment efficiency, proliferation and differentiation of bone marrow-derived mesenchymal stem/stromal cells (BMSCs) [111]. In particular, nano-HA allows a better adhesion, proliferation and differentiation of BMSCs into osteoblasts than ACP.

The chemical approach of creating functional groups on the surface of the scaffolds is also promising for the improvement of cell adhesion and osteogenic differentiation. For example, functional groups, such as –COOH and $–NH_2$, improve protein adsorption due to the formation of hydrogen bonds linking proteins, finally resulting in improved cell adhesion [97].

3.2. Enhancing the Mechanical Performance of Bioceramics Composites

CaP-based scaffolds generally exhibit poor mechanical properties compared to teeth and bone, especially due to their intrinsic brittleness, limiting their load-bearing bone applications [82,112]. Brittle materials are more likely to fail under tension or shearing rather than compression, essentially due to the crack propagation in preexisting flaws, such as micro-cracks or macro-pores [70,113].

Common approaches to improve mechanical performance and reduce the brittleness of ceramic materials are classified as intrinsic or extrinsic modifications (Figure 3).

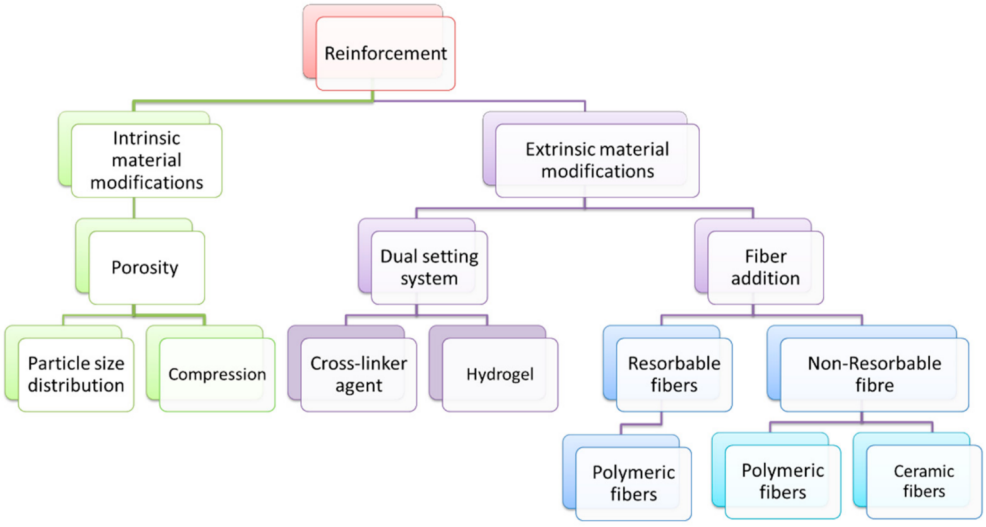

Figure 3. Mechanical reinforcement strategies for CaP-based biomaterials in a load-bearing application.

The intrinsic approach involves changes in the inherent properties of the scaffold, such as the composition, porosity and microstructure, whereas extrinsic modifications involve the use of reinforcing fibers or, in the case of CaP-based cements and pastes, the use of a cross-linker agent or hydrogel for the optimization of the dual setting system [72].

3.2.1. Intrinsic Material Modifications

The mechanical strength of scaffolds closely depends on their microstructure. Several factors, such as composition, crystal size and porosity, greatly affect the microstructure of scaffolds and its final strength [102]. One of the major factors affecting the mechanical performance is porosity, as the strength exponentially decreases with increasing voids [56,114,115].

A possible strategy to increase the mechanical strength is the reduction of intergranular voids by favoring the packing of the particles or using multimodal particle size distributions, leading to a decrease in the microporosity extent, especially in the struts [116].

The pore size distribution influences the degradation performance of the scaffold, and, therefore, the biodegradation kinetics can be modulated by varying the pore architecture [91]. Triangular, rectangular and elliptic pores were reported to support angiogenesis and faster cell migration due to their greater curvature [55]. Nevertheless, the increase in scaffold porosity is inversely related to mechanical strength; this is a key problem, difficult to solve and strongly limiting to load-bearing applications. In this respect, an exponential decrease in the compressive strength with increasing porosity was observed [115].

$$\sigma = [(E_0 R)/(\pi c)]^{0.5} \exp(-KP) \quad (2)$$

where E_0 is the Young's modulus at zero porosity; c is the average pore size; R is the fracture surface energy; K is an empirical constant, which can be extracted from the slope of a semi-logarithmic plot of the strength–porosity curve; and P is the porosity extent (in volume) [117,118].

Higher compressive moduli are associated with smaller pore sizes, porosity gradients and oriented pores [114,115]. The capability to modulate the porosity extent and distribution is helpful in limiting the concentration of mechanical stresses toward damage-tolerant structures; that is, micro-fractures occur until the scaffold's failure.

3.2.2. Extrinsic Material Modifications

The approaches proposed to increase the mechanical strength while limiting the brittleness of bioceramics include the combination with polymers, fibers or a dual setting system, especially for cements [104,107,108,119,120].

The dual setting system refers to the addition of reactive monomers to the liquid phase, together with an initiator into the inorganic component of the cement or eventually polymeric component that can be cross-linked [121,122]. In the first case, during the setting, there are simultaneous gelation/polymerization and dissolution–precipitation reactions, thus obtaining cement with a porous microstructure reinforced with a hydrogel-based matrix. As a consequence, an increase in compressive strength and hardness with stable rheological properties was achieved [102]. In turn, the cross-linking agent permits the binding of Ca^{2+} ions with carboxylic acid or organic phosphate fractions in the polymer chain, thus resulting in a reduction in brittleness and an increase in compressive strength [82,122].

The addition of fibers is one of the most effective approaches to increase the strength and toughness of bioceramics [123,124]. The mechanical behavior of fiber bioceramic composites is based on the interaction between the composite components and is time dependent due to the potential degradation of both fiber and CaP-based materials after implantation to allow bone regeneration. The reinforcements are related to several parameters, including (i) composition, mechanical properties and degradation of the matrix; (ii) fiber–matrix interface properties; and (iii) type, length, diameter, volume fraction, orientation and mechanical properties of fibers [124,125]. It was observed that the long-term strengthening effect of fibers was related to the type of fibers: the addition of non-resorbable fibers led to a stable increase in mechanical performance over time, while resorbable/biodegradable fibers provided only an initial reinforcement, followed by the creation of a macroporosity in the ceramic matrix after degradation of the fibers, favoring osteointegration [102].

The application of critical loads to brittle materials induces catastrophic fractures without any reversible deformation. The incorporation of fibers provides intergranular bridges increasing the tensile strength, flexural strength and fracture toughness.

There are three main fiber-reinforcing mechanisms [108,119,120]:

- Fiber bridging: the fibers bridge the existing crack, limiting its opening and propagation;
- Crack deflection: the fibers increase the length of the crack propagation, requiring more energy in newly formed surfaces;
- Frictional sliding: the presence of intergranular fibers in the matrix increases the fracture resistance of the composite.

Fibers can be classified as natural and man-made fibers, further divided into resorbable and non-resorbable [71] (Table 9).

Table 9. Fiber classification and some examples of fibers used in bioceramic reinforcement.

Natural Fibers	**Man-Made Fibers**			
	Resorbable		**Non-Resorbable**	
	Natural Polymer	Synthetic Polymer	Polymeric	Ceramics
Silk fibroin [107]	Polylactide [109] Cellulose [112]	Poly-caprolactone [109]	Polyamide [103,113]	Carbon [104,115,116,118] Silicate based [117,121,122,126] HA whiskers [122,127]

The introduction of carbon fibers (CF) in bioceramic scaffolds, including bone cements, has been explored in the past decades [123–125]. In particular, previous works showed that the addition of fibers led to an increase in compressive strength without interfering with HA formation during the setting of CPC [127]. The presence of CF induced a significant reinforcement also in calcinated HA-based scaffolds, while preserving biocompatibility and bioactivity; the mechanisms underlying the increase in mechanical properties were attributed to crack deflection, interlocking of the fibers, pullout and crack bridging [118]. Basically, the interaction between fibers and the surrounding ceramic matrix is based on

several properties of fibers, including chemical composition, wettability and surface modifications. HA bioceramics reinforced with silicon-coated CF with controllable alignment were prepared via hot pressing and pressureless sintering, leading to the formation of a SiO_2 protective layer upon thermal decomposition of HA [118].

Various oxidation treatments were also implemented to improve the performance of CF as a strengthening agent of CPCs, including a preliminary treatment with aqua regia followed by immersion in $CaCl_2$ [104]. This treatment favored the heterogeneous nucleation of apatite nanocrystals on the surface of fibers, thus reducing the setting times; the addition of 1 wt% of fibers led to a significant increase in both bending strength and the work of fracture, essentially due to the deflection of crack propagation, while the in vitro biocompatibility was preserved.

Moreover, silicate-based fibers, calcium silicate, glass and basalt fibers have been used to reinforce bioceramics [117,121,122,126]. In particular, wollastonite ($CaSiO_3$) fibers were introduced into CPCs, showing that Si could favor the crystallization of needle-like apatite during cement setting, associated with a significant increase in compressive strength [126]. Furthermore, the presence of $CaSiO_3$ fibers was a promoter of cell viability and ALP activity [121].

Glass fibers (GF), such as E-glass and bioactive glass fibers (BGF), have been proposed as CPC-reinforcing agents [128,129]. E-glass fibers are composed of alumino-borosilicate with about 1 wt% alkali oxides, while BGF is described by the ternary system SiO_2-CaO-P_2O_5 [122]. Xu and co-workers had incorporated short and long E-glass fibers into CPC, obtaining an increase in elastic modulus, flexural strength and the work of fracture [115]. The addition of 15 wt% of BGF also determined an improvement of compressive strength, toughness and elastic modulus of CPCs [122].

In addition to fibers, apatite whiskers were proposed to improve the mechanical properties of CPCs; the enhancement of 120% of the work of fracture and 60% of flexural strength was obtained by adding 30 vol% of HA whiskers [127].

4. Ion-Doped Bioceramics and Composite Scaffolds

4.1. Ion Doping

Calcium phosphates, especially HA, are capable of hosting a variety of foreign (i.e., different from Ca and P) ions, involving the formation of atomic defects but with a limited modification of the overall crystal structure [39]. As biological apatites forming the inorganic part of bone are characterized by nanocrystallinity, poor crystal ordering and multiple ion doping, in the last few decades, various approaches were proposed to tune the biological properties of ceramics [129–136] in order to obtain novel biomaterials with multifunctional abilities, including antibacterial [137–140] and magnetic properties [128].

Some of the most studied substituting ions in bioceramics, with related biological roles, are listed in Table 10.

Table 10. Doping ions in calcium phosphate bioceramics, with related biofunctional ability.

Ion	Biological Effects	References
Si^{4+}	- Induction of the biomimetic precipitation of HA - Osteogenic activity	[39,78,114]
Sr^{2+}	- Anti-osteoporotic agent - Enhancement of mechanical properties	[39,132,141]
Mg^{2+}	- Enhancement of bone growth - Induction of angiogenesis - Antibacterial agent	[39,132,139,141]

Table 10. *Cont.*

Ion	Biological Effects	References
Zn^{2+}	- Stimulation of osteoblastic activity - Inhibition of bone resorption - Antibacterial agent	[142–144]
Ag^{+}	- Antibacterial agent	[137,138,140]
Mn^{2+}	- Regulation of osteoblastic differentiation - Control of bone resorption - Promotion of cell adhesion - Promotion the synthesis of extracellular matrix proteins	[131,136]
Cu^{2+}	- Antibacterial agent	[131,136]
Co^{2+}	- Neo-vascularization promotion - High cell proliferation - Osteogenic activity	[131,136]
$Fe^{2+/3+}$	- Antibacterial agent - Super-paramagnetism - Promotion of bone formation - Osteoinductivity	[39,128,131,145]
F^{-}	- Shrinkage of HA crystal lattice - Decreasing solubilization and increasing stability of HA - Induction of biomineralization - Osteogenic activity - Antibacterial agent	[136,142,144,146,147]

4.1.1. Magnesium

Magnesium is considered as the main ion capable of replacing Ca in biological apatite, in an amount close to 1 wt% [132]. Mg^{2+} ions play a key role in bone metabolism, taking part of the biochemical reaction beyond bone formation, while also controlling bone growth and metabolism [47,142,148].

Magnesium phosphates are also associated with a higher dissolution rate than calcium phosphates [149]. Mg has been shown to inhibit the formation of crystalline minerals, such as hydroxyapatite, whereas more soluble phases, such as brushite, are minimally affected by the presence of Mg [150–152]. Specifically, it was observed in basic solutions that HAP precipitation is inhibited by Mg substitution for Ca higher than 10%, and amorphous calcium phosphate (ACP) or whitlockite, the Mg polymorph of β-tricalcium phosphate, forms [153,154].

The incorporation of magnesium was also associated with increased protein adsorption and cell adhesion on the surface of bioceramics [17,18]. Furthermore, an intrinsic antibacterial activity was described for Mg-HA [136,139].

4.1.2. Strontium

Strontium (Sr^{2+}) is a natural component of bones and teeth and have affinity with Ca^{2+} ions, thus representing a calcium-like entity within cells, acting along similar biochemical and cellular pathways [136,141]. At a low concentration, strontium inhibits osteoclast activity, reduces bone resorption, enhances osteoblast proliferation and promotes bone formation. In this context, the addition of strontium in bioceramics is promising for the local treatment of bone affected by metabolic diseases, such as osteoporosis [45,155–159]. Several approaches can be implemented to obtain Sr-doped bioceramics, including the addition of strontium salts in wet synthesis processes [160] or of Sr-doped inorganic reactants involved in solid-state reactions at high temperatures [73,159]. The incorporation of strontium ions replacing Ca^{2+} in the crystal lattice of calcium phosphates generally induces deformations in the crystal lattice due to its higher ionic radius in respect to calcium. This affects the physicochemical properties of CaPs; for instance, it was observed that Sr^{2+} ions stabilize the β-TCP polymorph during

thermal synthesis reactions. Furthermore, various previous studies reported a mechanical reinforcement ascribed to strontium doping, possibly due to enhancement of the interatomic bond strength in the CaP crystal in respect to calcium [161–163].

4.1.3. Silicon

Silicon plays a key role in the physiological formation of bone and cartilage tissues, especially due to its intrinsic capacity to act both as a cross-linker in ECM and to favor the precipitation of HA and bone mineralization [29,135]. When used in the synthesis of bioceramics, such as tricalcium phosphate (TCP), normally obtained with high-temperature treatments, silicon has the capacity to favor the formation of α-TCP polymorph against β-TCP [164,165]. Silicon-containing bioceramics exhibit high bioactivity, including bioglasses (Na-Ca-P-Si), wollastonite ($CaSiO_3$) and Si-doped bioceramics (e.g., Si-HA and Si-TCP) [24,27,29,32,48].

The pivotal role of Si-containing bioceramics, such as silicon-doped HA, in bone tissue regeneration was confirmed by in vivo studies revealing the enhanced formation of collagen fibrils after 6 weeks at the bone/Si-HA interface and after 12 weeks with the bone/HA interface [134,135]. In addition, the enhanced formation of mature osteoclasts from mononuclear precursor cells was observed, thus showing the potential of silicon to favor the complex bone regeneration cascade by stimulating the various cell lines involved in new bone formation and remodeling. Long-term in vivo studies also reported the significantly higher bioresorbability of Si-doped HA scaffolds compared to pure HA scaffolds, as only few residues of the doped scaffold were observed at one year upon implantation, while non-doped HA scaffolds remained unchanged even after five years from implantation [129].

4.1.4. Silver

The incorporation of silver ions into bioceramics, as a replacing element for calcium, is possible due to their similar ionic radius [133].

Silver doping has been proposed as a valuable antibacterial strategy due to its ability to interfere with the electron transfer process on bacterial membranes and to promote the production of reactive oxygen species (ROS), finally causing cell death [148].

4.1.5. Iron

The incorporation of iron ions into bioceramics has been widely studied in recent decades, together with its neighboring transition elements from the fourth period of the periodic table (Mn, Co, Ni, Zn) [39], with the purpose of generating new bioceramics with magnetic properties. Indeed, super-paramagnetic iron oxide nanoparticles (SPIONs) are widely approved magnetic biomaterials (usually composed of magnetite Fe_3O_4 or maghemite γ-Fe_2O_3) as a contrast agent in magnetic resonance imaging applications for cancer diagnosis or hyperthermia-based cancer treatments. Nevertheless, their iron oxide core also causes long-term cytotoxicity; therefore, intensive effort is today dedicated to develop iron-doped magnetic ceramics preserving good biocompatibility and bioactivity [166].

In this respect, iron-doped CPCs for magnetic hyperthermia were obtained, exhibiting improved osteoconductive and antibacterial properties [167–169]. A new concept of magnetic CaP was obtained by synthesizing apatite nanocrystals doped with $Fe^{2+/3+}$ ions, so as to generate intrinsic superparamagnetic ability, generated by the specific positioning of Fe^{2+} and Fe^{3+} ions in the crystal lattice and in the outer hydrated layer of the apatite [128,145]. Such a new phase exhibited a magnetization ability similar to that of iron oxides but with excellent biocompatibility and enhanced osteogenic ability [170].

4.1.6. Fluorine

Fluorine ions take part in several biochemical processes, becoming particularly important for oral care applications, neuromodulation and bone structure [136]. Fluorine pro-

motes osteoblast proliferation and inhibits osteoclast activation and differentiation; moreover, when present in a low concentration, it can enhance in vivo bone formation [147,171].

The substitution of OH^- groups of apatite with F^- ions accelerated the crystallization process, increasing the stability of the crystals while decreasing their solubility [147,171]; the incorporation of fluorine also affected the crystal morphology toward flattened hexagonal rod-like shapes [147,171].

Fluorine-doped HA also exhibited antibacterial behavior, inhibiting the adhesion and proliferation of bacteria typically detected in an oral environment [147,171].

4.2. Composites with Silicates

The preparation of composites containing both calcium phosphates and silicates has been explored with several approaches for the purpose of enhancing the mechanical properties of scaffolds. In fact, various studies showed that calcium phosphate composites with calcium silicates exhibited enhanced compressive and flexural strength [172,173].

Si-containing bioceramics include colloidal silica nanoparticles [174,175], silicates (i.e., calcium silicates and zinc silicates) [176–178], glasses [179,180] and silicate-phosphates (i.e., silicocarnotite and nagelschmidtite) [181,182]. Regarding the preparation of bone cements, previous studies showed that the addition of silica nanoparticles led to a decrease in the setting times and led to improved mechanical properties, especially due to the formation of Si-O-Si bonds among the particles [174,175]. Calcium phosphate cements containing zinc silicate and PLGA microspheres were also prepared [162]: the role of Si and Zn in improving setting times, injectability and compression strength was observed, while the addition of the microspheres did not affect the porosity.

The incorporation of silicates becomes particularly interesting in bioglass-reinforced cements, e.g., single-phase crystalline or amorphous calcium silicate phosphates ($CaO\text{-}SiO_2\text{-}P_2O_5$, CaSiP) or Bioglass A5S4, resulting in increased setting times and injectability [179,180]. The incorporation of bioglasses also significantly improved the bioactivity of the scaffold, promoting osteoblast attachment, proliferation and differentiation in vivo. The effect of CaSiP (silicocarnotite, $Ca_5(PO_4)_2SiO_4$) in brushite cements was also investigated, showing the role of Si in favoring the formation of HA, osteoblast proliferation and the formation of novel bone tissue [181].

The application of single-phase calcium phosphate silicate bioceramics (CaSiP) is not limited to bone regeneration but also to periodontal repair. In this respect, various works showed the preparation of 3D-printed silicate bioceramics, such as nagelschmidtite ($Ca_7(SiO_4)_3(PO_4)_2$, CSP) and silicocarnotite ($Ca_5(PO_4)_2SiO_4$, S_{ss}) [48]. CaSiP showed good biological performance with the formation of flake-like apatite layers (in the cases of S_{ss} and CSP, respectively). The ion release positively induced cell proliferation and differentiation as well as the formation of the extracellular matrix and the mineralization of periodontal tissue [183,184].

4.3. Composites with Carbon

The interest in the synthesis of composites with calcium phosphates and carbon-derived structures rapidly rose in recent years, especially considering graphene, a 2D material made of nanosheets of hexagonally bonded carbon atoms characterized by a high surface area, high conductivity, excellent mechanical properties and good biocompatibility, particularly interesting for tissue engineering applications [185–187].

The synthesis strategies to obtain graphene/carbon nanotubes–hydroxyapatite composites have been reported, evidencing hemocompatibility, antibacterial properties and the ability of graphene–hydroxyapatite composites to increase osteogenic activity [161,163,188–194].

A hybrid composite made of graphene oxide (GO), chitosan (CS) and HA (GO-CS-HA) was developed as a coating for titanium implants, exhibiting an increased formation of biomimetic apatite and also antibacterial properties, possibly ascribed to the increased production of reactive oxygen species [177].

Furthermore, 3D-printed composite scaffolds made of β-TCP, reduced graphene oxide (RGO), magnesium nanoparticles and arginine were prepared [176]. The combination of amino groups of arginine, released Mg ions and the nanotopography of GO resulted in increased mechanical performance.

The effect of RGO and carbon nanotubes (CNT) in α-TCP-based cements was evaluated. The setting times decreased when increasing the concentration of RGO, while negligible variations were observed with the addition of CNT; the mechanical performance was also valuable for load-bearing applications [178,195].

The use of microwaves resulted in a reduction in setting time and an increase in mechanical properties, ascribed to the evaporation of gas from the surface of RGO and CNT, strengthening the final composite [195]. The formation of an external HA layer was observed, favoring cell adhesion and proliferation.

4.4. Composites with Titanates

Titanium and its alloys have been used in combination with calcium phosphates for bone tissue engineering due to their excellent mechanical properties [196]. Metallic prostheses and implants are widely used to replace damaged bones and teeth, and their interaction with the surrounding tissue depends on the chemistry and microstructure of the surface [197], but their main drawback is related to their poor bioresorbability. In this respect, the preparation of bioceramic composites containing titanium oxides was considered as a valuable approach, exhibiting good biocompatibility and enhancing in vivo osteointegration [198,199].

Titanium oxide nanomaterials can also be added to injectable cements and pastes, leading to higher injectability and improved mechanical performance [175].

Some titanates, such as barium titanate ($BaTiO_3$, BT) and strontium titanate ($SrTiO_3$), are also characterized by piezoelectric properties, potentially providing microstructural accumulation of charges mimicking the mechanotransduction of bone cells [183,184,200,201]. BT-HA composites were investigated to combine the bioactivity of HA with the piezoelectricity of BT [184,200]. Three-dimensional-printed highly porous piezoelectric scaffolds based on BT and HA were obtained, with good cytocompatibility and cell attachment [184]. An aligned porous BT-HA piezoelectric composite was obtained by the ice-template method, exhibiting high porosity, cell proliferation, differentiation and adhesion of osteoblastic cells [200].

5. Conclusions

Calcium phosphates are widely accepted biomaterials and the gold standard to promote the regeneration of bone tissue. CaP scaffolds with biomimetic composition can exhibit osteogenic ability, bioresorbability and antibacterial properties. However, appropriate mechanical properties are required if the target is the regeneration of critical-sized bone defects, particularly when load bearing.

The co-existence of various factors, such as bioactive chemical composition, nanostructure and bone-like mechanical performance, is a major problem with ceramics due to the need of sintering and the difficulty of achieving complex bone-mimicking 3D structures. In fact, several technologies developed in the last decades for the manufacturing of a highly porous bioceramic-based scaffold from traditional methods (partial sintering, replica method, sacrificial template and direct foaming, as well as various 3D printing technologies) usually fail in generating bioactive and effective bone scaffolds. Hence, future perspectives are strongly related to the development of new approaches that can generate bone scaffolds endowed with bone-mimicking features yielding effective regenerative ability. To this end, recently developed innovative approaches targeting low-temperature processes, including chemically induced consolidation of CaP pastes or biomorphic transformation processes, are examples of radically new methods enabling the possibility to create scaffolds retaining nanocrystallinity and bioactive, ion-doped composition or even multi-scale hierarchically organized architectures inherited from natural sources. These

results open new perspectives in ceramic science and are encouraging for further research in the field, targeting the decisive resolution of many still unmet clinical problems related to bone regeneration.

Author Contributions: Conceptualization, S.S., A.T. and M.D.; methodology, S.S., A.T. and M.D.; writing—original draft preparation, M.T.; writing—review and editing, M.D.; supervision, M.D. and S.S.; All authors have read and agreed to the published version of the manuscript.

Funding: This research received no external funding.

Conflicts of Interest: The authors declare no conflict of interest.

References

1. Bean, A.C. Basic Science Concepts in Musculoskeletal Regenerative Medicine. In *Regenerative Medicine for Spine and Joint Pain*; Springer: Berlin/Heidelberg, Germany, 2020; pp. 5–27. [CrossRef]
2. Li, J.J.; Ebied, M.; Xu, J.; Zreiqat, H. Current Approaches to Bone Tissue Engineering: The Interface between Biology and Engineering. *Adv. Healthc. Mater.* **2018**, *7*, 1–8. [CrossRef] [PubMed]
3. Sommerfeldt, D.; Rubin, C. Biology of bone and how it orchestrates the form and function of the skeleton. *Eur. Spine J.* **2001**, *10*, 86–95. [CrossRef]
4. Armiento, A.R.; Hatt, L.P.; Sanchez Rosenberg, G.; Thompson, K.; Stoddart, M.J. Functional Biomaterials for Bone Regeneration: A Lesson in Complex Biology. *Adv. Funct. Mater.* **2020**, *1909874*, 1–41. [CrossRef]
5. Berthiaume, F.; Maguire, T.J.; Yarmush, M.L. Tissue Engineering and Regenerative Medicine: History, Progress, and Challenges. *Annu. Rev. Chem. Biomol. Eng.* **2011**, *2*, 403–430. [CrossRef] [PubMed]
6. Cooper, G.; Herrera, J.; Kirkbride, J.; Perlman, Z. Introduction to Regenerative Medicine. In *Regenerative Medicine for Spine and Joint Pain*; Springer: Berlin/Heidelberg, Germany, 2020; pp. 1–4. [CrossRef]
7. Oryan, A.; Alidadi, S.; Moshiri, A.; Maffulli, N. Bone regenerative medicine: Classic options, novel strategies, and future directions. *J. Orthop. Surg. Res.* **2014**, *9*, 1–27. [CrossRef]
8. Vaish, A.; Murrell, W.; Vaishya, R. History of regenerative medicine in the field of orthopedics. *J. Arthrosc. Surg. Sports Med.* **2020**, *1*, 154–158. [CrossRef]
9. Eliaz, N.; Metoki, N. Calcium phosphate bioceramics: A review of their history, structure, properties, coating technologies and biomedical applications. *Materials* **2017**, *10*, 334. [CrossRef] [PubMed]
10. Jodati, H.; Bengi, Y.; Evis, Z. A review of bioceramic porous sca ff olds for hard tissue applications: Effects of structural features. *Ceram. Int.* **2020**, *46*, 15725–15739. [CrossRef]
11. Pereira, H.F.; Cengiz, I.F.; Samuel, F.; Rui, S.; Reis, L.; Oliveira, J.M. Scaffolds and coatings for bone regeneration. *J. Mater. Sci. Mater. Med.* **2020**, *31*, 27. [CrossRef]
12. Williams, D.F. On the mechanisms of biocompatibility. *Biomaterials* **2008**, *29*, 2941–2953. [CrossRef]
13. Polo-Corrales, L.; Latorre-Esteves, M.; Ramirez-Vick, J.E. Scaffold design for bone regeneration. *J. Nanosci. Nanotechnol.* **2014**, *14*, 15–56. [CrossRef] [PubMed]
14. Kielty, C.M.; Grant, M.E. The Collagen Family: Structure, Assembly, and Organization in the Extracellular Matrix. In *Connective Tissue and Its Heritable Disorders*; Wiley: Hoboken, NJ, USA, 2003; pp. 159–221. [CrossRef]
15. No, Y.J.; Holzmeister, I.; Lu, Z.; Prajapati, S.; Shi, J.; Gbureck, U.; Zreiqat, H. Effect of baghdadite substitution on the physicochemical properties of brushite cements. *Materials* **2019**, *12*, 1719. [CrossRef] [PubMed]
16. Jeong, J.; Kim, J.H.; Shim, J.H.; Hwang, N.S.; Heo, C.Y. Bioactive calcium phosphate materials and applications in bone regeneration. *Biomater. Res.* **2019**, *23*, 1–11. [CrossRef] [PubMed]
17. Tampieri, A.; Iafisco, M.; Sprio, S.; Ruffini, A.; Panseri, S.; Montesi, M.; Adamiano, A.; Sandri, M. Hydroxyapatite: From Nanocrystals to Hybrid Nanocomposites for Regenerative Medicine. In *Handbook of Bioceramics and Biocomposites*; Springer: Berlin/Heidelberg, Germany, 2016; pp. 119–144. [CrossRef]
18. Sprio, S.; Sandri, M.; Iafisco, M.; Panseri, S.; Filardo, G.; Kon, E.; Marcacci, M.; Tampieri, A. Composite biomedical foams for engineering bone tissue. In *Biomedical Foams for Tissue Engineering Applications*; Woodhead Publishing: Sawston, UK, 2014; pp. 249–280. [CrossRef]
19. Barrère, F.; van Blitterswijk, C.A.; de Groot, K. Bone regeneration: Molecular and cellular interactions with calcium phosphate ceramics. *Int. J. Nanomed.* **2006**, *1*, 317–332.
20. Sprio, S.; Ruffini, A.; Valentini, F.; D'Alessandro, T.; Sandri, M.; Panseri, S.; Tampieri, A. Biomimesis and biomorphic transformations: New concepts applied to bone regeneration. *J. Biotechnol.* **2011**, *156*, 347–355. [CrossRef]
21. Wegst, U.G.K.; Bai, H.; Saiz, E.; Tomsia, A.P.; Ritchie, R.O. Bioinspired structural materials. *Nature* **2015**, *14*, 23–36. [CrossRef]
22. Rho, J.Y.; Kuhn-Spearing, L.; Zioupos, P. Mechanical properties and the hierarchical structure of bone. *Med. Eng. Phys.* **1998**, *20*, 92–102. [CrossRef]
23. Kang, J.; Dong, E.; Li, D.; Dong, S.; Zhang, C.; Wang, L. Anisotropy characteristics of microstructures for bone substitutes and porous implants with application of additive manufacturing in orthopaedic. *Mater. Des.* **2020**, *191*, 108608. [CrossRef]

24. Arcos, D.; Vallet-Regí, M. Sol-gel silica-based biomaterials and bone tissue regeneration. *Acta Biomater.* **2010**, *6*, 2874–2888. [CrossRef]
25. Burdușel, A.-C. Bioactive composites for bone regeneration. *Biomed. Eng. Int.* **2019**, *1*, 9–15. [CrossRef]
26. Fernandez de Grado, G.; Keller, L.; Idoux-Gillet, Y.; Wagner, Q.; Musset, A.M.; Benkirane-Jessel, N.; Bornert, F.; Offner, D. Bone substitutes: A review of their characteristics, clinical use, and perspectives for large bone defects management. *J. Tissue Eng.* **2018**, *9*, 2041731418776819. [CrossRef] [PubMed]
27. Lei, Q.; Guo, J.; Noureddine, A.; Wang, A.; Wuttke, S.; Brinker, C.J.; Zhu, W. Sol–Gel-Based Advanced Porous Silica Materials for Biomedical Applications. *Adv. Funct. Mater.* **2020**, *1909539*, 1–28. [CrossRef]
28. Shue, L.; Yufeng, Z.; Mony, U. Biomaterials for periodontal regeneration A review of ceramics and polymers. *BioMatter* **2012**, *2*, 271–277. [CrossRef]
29. Venkatraman, S.K.; Swamiappan, S. Review on calcium- and magnesium-based silicates for bone tissue engineering applications. *J. Biomed. Mater. Res. Part A* **2020**, *108*, 1546–1562. [CrossRef]
30. Yousefi, A.-M. A review of calcium phosphate cements and acrylic bone cements as injectable materials for bone repair and implant fixation. *J. Appl. Biomater. Funct. Mater.* **2019**, *17*, 228080001987259. [CrossRef] [PubMed]
31. Yamamuro, T. Bioceramics. In *Biomechanics and Biomaterials in Orthopedics*; Springer: Berlin/Heidelberg, Germany, 2004; pp. 22–33. [CrossRef]
32. Gul, H.; Khan, M.; Khan, A.S. 3—Bioceramics: Types and clinical applications. In *Handbook of Ionic Substituted Hydroxyapatites*; Elsevier: Amsterdam, The Netherlands, 2020; pp. 53–83. [CrossRef]
33. Li, X.; Wang, J.; Joiner, A.; Chang, J. The remineralisation of enamel: A review of the literature. *J. Dent.* **2014**, *42*, S12–S20. [CrossRef]
34. Doremus, R.H. Review Bioceramics. *J. Mater. Sci.* **1992**, *27*, 285–297. [CrossRef]
35. Low, K.L.; Tan, S.H.; Zein, S.H.S.; Roether, J.A.; Mouriño, V.; Boccaccini, A.R. Calcium phosphate-based composites as injectable bone substitute materials. *J. Biomed. Mater. Res. Part B Appl. Biomater.* **2010**, *94*, 273–286. [CrossRef]
36. Surmenev, R.A.; Surmeneva, M.A.; Ivanova, A.A. Significance of calcium phosphate coatings for the enhancement of new bone osteogenesis—A review. *Acta Biomater.* **2014**, *10*, 557–579. [CrossRef]
37. Kucko, N.W.; Herber, R.-P.; Leeuwenburgh, S.C.G.; Jansen, J.A. Calcium Phosphate Bioceramics and Cements. In *Principles of Regenerative Medicine*; Elsevier: Amsterdam, The Netherlands, 2019; pp. 591–611. [CrossRef]
38. Ginebra, M.P.; Espanol, M.; Maazouz, Y.; Bergez, V.; Pastorino, D. Bioceramics and bone healing. *EFORT Open Rev.* **2018**, *3*, 173–183. [CrossRef]
39. Uskoković, V. Ion-doped hydroxyapatite: An impasse or the road to follow? *Ceram. Int.* **2020**, *46*, 11443–11465. [CrossRef]
40. Graziani, G.; Boi, M.; Bianchi, M. A review on ionic substitutions in hydroxyapatite thin films: Towards complete biomimetism. *Coatings* **2018**, *8*, 269. [CrossRef]
41. Carrodeguas, R.G.; De Aza, S. α-Tricalcium phosphate: Synthesis, properties and biomedical applications. *Acta Biomater.* **2011**, *7*, 3536–3546. [CrossRef] [PubMed]
42. Lobo, S.E.; Livingston Arinzeh, T. Biphasic Calcium Phosphate Ceramics for Bone Regeneration and Tissue Engineering Applications. *Materials* **2010**, *3*, 815–826. [CrossRef]
43. Maji, K.; Mondal, S. Calcium Phosphate Biomaterials for Bone Tissue Engineering: Properties and Relevance in Bone Repair. In *Racing for the Surface: Antimicrobial and Interface Tissue Engineering*; Springer: Berlin/Heidelberg, Germany, 2020; pp. 535–555. [CrossRef]
44. Cabrejos-Azama, J.; Alkhraisat, M.H.; Rueda, C.; Torres, J.; Blanco, L.; López-Cabarcos, E. Magnesium substitution in brushite cements for enhanced bone tissue regeneration. *Mater. Sci. Eng. C* **2014**, *43*, 403–410. [CrossRef]
45. Pina, S.; Ferreira, J.M.F. Brushite-forming Mg-, Zn- and Sr-substituted bone cements for clinical applications. *Materials* **2010**, *3*, 519–535. [CrossRef]
46. Theiss, F.; Apelt, D.; Brand, B.; Kutter, A.; Zlinszky, K.; Bohner, M.; Matter, S.; Frei, C.; Auer, J.A.; Von Rechenberg, B. Biocompatibility and resorption of a brushite calcium phosphate cement. *Biomaterials* **2005**, *26*, 4383–4394. [CrossRef]
47. Huan, Z.; Chang, J. Novel bioactive composite bone cements based on the β-tricalcium phosphate-monocalcium phosphate monohydrate composite cement system. *Acta Biomater.* **2009**, *5*, 1253–1264. [CrossRef] [PubMed]
48. Sepantafar, M.; Mohammadi, H.; Maheronnaghsh, R.; Tayebi, L.; Baharvand, H. Single phased silicate-containing calcium phosphate bioceramics: Promising biomaterials for periodontal repair. *Ceram. Int.* **2018**, *44*, 11003–11012. [CrossRef]
49. Jablonská, E.; Horkavcová, D.; Rohanová, D.; Brauer, D.S. A review of: In vitro cell culture testing methods for bioactive glasses and other biomaterials for hard tissue regeneration. *J. Mater. Chem. B* **2020**, *8*, 10941–10953. [CrossRef]
50. Hench, L.L.; Jones, J.R. Bioactive glasses: Frontiers and Challenges. *Front. Bioeng. Biotechnol.* **2015**, *3*, 1–12. [CrossRef]
51. Prasadh, S.; Wong, R.C.W. Unraveling the mechanical strength of biomaterials used as a bone scaffold in oral and maxillofacial defects. *Oral Sci. Int.* **2018**, *15*, 48–55. [CrossRef]
52. Roseti, L.; Parisi, V.; Petretta, M.; Cavallo, C.; Desando, G.; Bartolotti, I.; Grigolo, B. Scaffolds for Bone Tissue Engineering: State of the art and new perspectives. *Mater. Sci. Eng. C* **2017**, *78*, 1246–1262. [CrossRef] [PubMed]
53. Peroglio, M.; Gremillard, L.; Chevalier, J.; Chazeau, L.; Gauthier, C.; Hamaide, T. Toughening of bio-ceramics scaffolds by polymer coating. *J. Eur. Ceram. Soc.* **2007**, *27*, 2679–2685. [CrossRef]
54. Steinbrech, R.W. Toughening mechanisms for ceramic materials. *J. Eur. Ceram. Soc.* **1992**, *10*, 131–142. [CrossRef]

55. Abbasi, N.; Hamlet, S.; Love, R.M.; Nguyen, N.T. Porous scaffolds for bone regeneration. *J. Sci. Adv. Mater. Devices* **2020**, *5*, 1–9. [CrossRef]
56. Studart, A.R.; Gonzenbach, U.T.; Tervoort, E.; Gauckler, L.J. Processing routes to macroporous ceramics: A review. *J. Am. Ceram. Soc.* **2006**, *89*, 1771–1789. [CrossRef]
57. Champion, E. Sintering of calcium phosphate bioceramics. *Acta Biomater.* **2013**, *9*, 5855–5875. [CrossRef]
58. Eom, J.H.; Kim, Y.W.; Raju, S. Processing and properties of macroporous silicon carbide ceramics: A review. *J. Asian Ceram. Soc.* **2013**, *1*, 220–242. [CrossRef]
59. Kim, I.J.; Park, J.G.; Han, Y.H.; Kim, S.Y.; Shackelford, J.F. Wet foam stability from colloidal suspension to porous ceramics: A review. *J. Korean Ceram. Soc.* **2019**, *56*, 211–232. [CrossRef]
60. Ohji, T.; Fukushima, M. Macro-porous ceramics: Processing and properties. *Int. Mater. Rev.* **2012**, *57*, 115–131. [CrossRef]
61. Dapporto, M.; Sprio, S.; Fabbi, C.; Figallo, E.; Tampieri, A. A novel route for the synthesis of macroporous bioceramics for bone regeneration. *J. Eur. Ceram. Soc.* **2016**, *36*, 2383–2388. [CrossRef]
62. Deville, S. Freeze-casting of porous ceramics: A review of current achievements and issues. *Adv. Eng. Mater.* **2008**, *10*, 155–169. [CrossRef]
63. Babaie, E.; Bhaduri, S.B. Fabrication Aspects of Porous Biomaterials in Orthopedic Applications: A Review. *ACS Biomater. Sci. Eng.* **2018**, *4*, 1–39. [CrossRef] [PubMed]
64. Ginebra, M.P. Cements as bone repair materials. In *Bone Repair Biomaterials*; Elsevier: Amsterdam, The Netherlands, 2009; pp. 271–308. [CrossRef]
65. Lewis, G. Injectable bone cements for use in vertebroplasty and kyphoplasty: State-of-the-art review. *J. Biomed. Mater. Res. Part B Appl. Biomater.* **2006**, *76*, 456–468. [CrossRef]
66. Şahin, E.; Kalyon, D.M. The rheological behavior of a fast-setting calcium phosphate bone cement and its dependence on deformation conditions. *J. Mech. Behav. Biomed. Mater.* **2017**, *72*, 252–260. [CrossRef] [PubMed]
67. Vaishya, R.; Chauhan, M.; Vaish, A. Bone cement. *J. Clin. Orthop. Trauma* **2013**, *4*, 157–163. [CrossRef]
68. Ginebra, M.P.; Canal, C.; Espanol, M.; Pastorino, D.; Montufar, E.B. Calcium phosphate cements as drug delivery materials. *Adv. Drug Deliv. Rev.* **2012**, *64*, 1090–1110. [CrossRef]
69. O'Neill, R.; McCarthy, H.O.; Montufar, E.B.; Ginebra, M.P.; Wilson, D.I.; Lennon, A.; Dunne, N. Critical review: Injectability of calcium phosphate pastes and cements. *Acta Biomater.* **2017**, *50*, 1–19. [CrossRef]
70. Zhang, J.; Liu, W.; Schnitzler, V.; Tancret, F.; Bouler, J.M. Calcium phosphate cements for bone substitution: Chemistry, handling and mechanical properties. *Acta Biomater.* **2014**, *10*, 1035–1049. [CrossRef]
71. Canal, C.; Ginebra, M.P. Fibre-reinforced calcium phosphate cements: A review. *J. Mech. Behav. Biomed. Mater.* **2011**, *4*, 1658–1671. [CrossRef]
72. Bigi, A.; Boanini, E. Functionalized biomimetic calcium phosphates for bone tissue repair. *J. Appl. Biomater. Funct. Mater.* **2017**, *15*, e313–e325. [CrossRef] [PubMed]
73. Dapporto, M.; Gardini, D.; Tampieri, A.; Sprio, S. Nanostructured Strontium-Doped Calcium Phosphate Cements: A Multifactorial Design. *Appl. Sci.* **2021**, *11*, 2075. [CrossRef]
74. International Organization for Standardization. *Implants for Surgery—Calcium Phosphate Bioceramics—Characterization of Hardening Bone Paste Materials—ISO/DIS 18531(en)*; ISO: Geneva, Switzerland, 2015.
75. Baino, F.; Ferraris, M. Learning from Nature: Using bioinspired approaches and natural materials to make porous bioceramics. *Int. J. Appl. Ceram. Technol.* **2017**, *14*, 507–520. [CrossRef]
76. Sprio, S.; Panseri, S.; Montesi, M.; Dapporto, M.; Ruffini, A.; Dozio, S.M.; Cavuoto, R.; Misseroni, D.; Paggi, M.; Bigoni, D.; et al. Hierarchical porosity inherited by natural sources affects the mechanical and biological behaviour of bone scaffolds. *J. Eur. Ceram. Soc.* **2020**, *40*, 1717–1727. [CrossRef]
77. Tampieri, A.; Sprio, S.; Ruffini, A.; Celotti, G.; Lesci, I.G.; Roveri, N. From wood to bone: Multi-step process to convert wood hierarchical structures into biomimetic hydroxyapatite scaffolds for bone tissue engineering. *J. Mater. Chem.* **2009**, *19*, 4973–4980. [CrossRef]
78. Lucas-Aparicio, J.; Manchón, Á.; Rueda, C.; Pintado, C.; Torres, J.; Alkhraisat, M.H.; López-Cabarcos, E. Silicon-calcium phosphate ceramics and silicon-calcium phosphate cements: Substrates to customize the release of antibiotics according to the idiosyncrasies of the patient. *Mater. Sci. Eng. C* **2020**, *106*, 110173. [CrossRef]
79. Sprio, S.; Sandri, M.; Iafisco, M.; Panseri, S.; Adamiano, A.; Montesi, M.; Campodoni, E.; Tampieri, A. Bio-inspired assembling/mineralization process as a flexible approach to develop new smart scaffolds for the regeneration of complex anatomical regions. *J. Eur. Ceram. Soc.* **2016**, *36*, 2857–2867. [CrossRef]
80. Vincent, J.F.V.; Bogatyreva, O.A.; Bogatyrev, N.R.; Bowyer, A.; Pahl, A.K. Biomimetics: Its practice and theory. *J. R. Soc. Interface* **2006**, *3*, 471–482. [CrossRef]
81. White, R.A.; Weber, J.N.; White, E.W. Replamineform: A new process for preparing porous ceramic, metal, and polymer prosthetic materials. *Science* **1972**, *176*, 922–924. [CrossRef] [PubMed]
82. Tampieri, A.; Ruffini, A.; Ballardini, A.; Montesi, M.; Panseri, S.; Salamanna, F.; Fini, M.; Sprio, S. Heterogeneous chemistry in the 3-D state: An original approach to generate bioactive, mechanically-competent bone scaffolds. *Biomater. Sci.* **2019**, *7*, 307–321. [CrossRef]

83. Guvendiren, M.; Molde, J.; Soares, R.M.D.; Kohn, J. Designing Biomaterials for 3D Printing. *ACS Biomater. Sci. Eng.* **2016**, *2*, 1679–1693. [CrossRef]
84. Hart, L.R.; He, Y.; Ruiz-Cantu, L.; Zhou, Z.; Irvine, D.; Wildman, R.; Hayes, W. 3D and 4D printing of biomaterials and biocomposites, bioinspired composites, and related transformers. In *3D and 4D Printing of Polymer Nanocomposite Materials: Processes, Applications, and Challenges*; Elsevier: Amsterdam, The Netherlands, 2019; pp. 467–504. [CrossRef]
85. Ngo, T.D.; Kashani, A.; Imbalzano, G.; Nguyen, K.T.Q.; Hui, D. Additive manufacturing (3D printing): A review of materials, methods, applications and challenges. *Compos. Part B Eng.* **2018**, *143*, 172–196. [CrossRef]
86. Wang, X.; Peng, X.; Yue, P.; Qi, H.; Liu, J.; Li, L.; Guo, C.; Xie, H.; Zhou, X.; Yu, X. A novel CPC composite cement reinforced by dopamine coated SCPP fibers with improved physicochemical and biological properties. *Mater. Sci. Eng. C* **2020**, *109*. [CrossRef]
87. Bose, S.; Robertson, S.F.; Bandyopadhyay, A. Surface modification of biomaterials and biomedical devices using additive manufacturing. *Acta Biomater.* **2018**, *66*, 6–22. [CrossRef]
88. Chen, Z.; Li, Z.; Li, J.; Liu, C.; Lao, C.; Fu, Y.; Liu, C.; Li, Y.; Wang, P.; He, Y. 3D printing of ceramics: A review. *J. Eur. Ceram. Soc.* **2019**, *39*, 661–687. [CrossRef]
89. Ghorbani, F.; Li, D.; Ni, S.; Zhou, Y.; Yu, B. 3D printing of acellular scaffolds for bone defect regeneration: A review. *Mater. Today Commun.* **2020**, *22*, 100979. [CrossRef]
90. Sinha, S.K. Additive manufacturing (AM) of medical devices and scaffolds for tissue engineering based on 3D and 4D printing. In *3D and 4D Printing of Polymer Nanocomposite Materials: Processes, Applications, and Challenges*; Elsevier: Amsterdam, The Netherlands, 2019; pp. 119–160. [CrossRef]
91. Ma, H.; Feng, C.; Chang, J.; Wu, C. 3D-printed bioceramic scaffolds: From bone tissue engineering to tumor therapy. *Acta Biomater.* **2018**, *79*, 37–59. [CrossRef] [PubMed]
92. Stevens, M.M. Biomaterials for bone tissue engineering. *Mater. Today* **2008**, *11*, 18–25. [CrossRef]
93. Wang, C.; Huang, W.; Zhou, Y.; He, L.; He, Z.; Chen, Z.; He, X.; Tian, S.; Liao, J.; Lu, B.; et al. 3D printing of bone tissue engineering scaffolds. *Bioact. Mater.* **2020**, *5*, 82–91. [CrossRef]
94. Mondal, S.; Nguyen, T.P.; Pham, V.H.; Hoang, G.; Manivasagan, P.; Kim, M.H.; Nam, S.Y.; Oh, J. Hydroxyapatite nano bioceramics optimized 3D printed poly lactic acid scaffold for bone tissue engineering application. *Ceram. Int.* **2020**, *46*, 3443–3455. [CrossRef]
95. Pina, S.; Ribeiro, V.P.; Marques, C.F.; Maia, F.R.; Silva, T.H.; Reis, R.L.; Oliveira, J.M. Scaffolding Strategies for Tissue Engineering and Regenerative Medicine Applications. *Materials* **2019**, *12*, 1824. [CrossRef] [PubMed]
96. Xiao, D.; Zhang, J.; Zhang, C.; Barbieri, D.; Yuan, H.; Moroni, L.; Feng, G. The role of calcium phosphate surface structure in osteogenesis and the mechanisms involved. *Acta Biomater.* **2020**, *106*, 22–33. [CrossRef] [PubMed]
97. Zhu, L.; Luo, D.; Liu, Y. Effect of the nano/microscale structure of biomaterial scaffolds on bone regeneration. *International J. Oral Sci.* **2020**, *12*, 1–15. [CrossRef]
98. Tarafder, S.; Dernell, W.S.; Bandyopadhyay, A.; Bose, S. SrO- and MgO-doped microwave sintered 3D printed tricalcium phosphate scaffolds: Mechanical properties and in vivo osteogenesis in a rabbit model. *J. Biomed. Mater. Res. Part B Appl. Biomater.* **2015**, *103*, 679–690. [CrossRef]
99. Touri, M.; Moztarzadeh, F.; Abu Osman, N.A.; Dehghan, M.M.; Brouki Milan, P.; Farzad-Mohajeri, S.; Mozafari, M. Oxygen-Releasing Scaffolds for Accelerated Bone Regeneration. *ACS Biomater. Sci. Eng.* **2020**, *6*, 2985–2994. [CrossRef]
100. Sun, H.; Hu, C.; Zhou, C.; Wu, L.; Sun, J.; Zhou, X.; Xing, F.; Long, C.; Kong, Q.; Liang, J.; et al. 3D printing of calcium phosphate scaffolds with controlled release of antibacterial functions for jaw bone repair. *Mater. Des.* **2020**, *189*, 108540. [CrossRef]
101. Liu, D.; Nie, W.; Li, D.; Wang, W.; Zheng, L.; Zhang, J.; Zhang, J.; Peng, C.; Mo, X.; He, C. 3D printed PCL/SrHA scaffold for enhanced bone regeneration. *Chem. Eng. J.* **2019**, *362*, 269–279. [CrossRef]
102. Geffers, M.; Groll, J.; Gbureck, U. Reinforcement strategies for load-bearing calcium phosphate biocements. *Materials* **2015**, *8*, 2700–2717. [CrossRef]
103. Xu, H.H.K.; Quinn, J.B.; Takagi, S.; Chow, L.C.; Eichmiller, F.C. Strong and macroporous calcium phosphate cement: Effects of porosity and fiber reinforcement on mechanical properties. *J. Biomed. Mater. Res.* **2001**, *57*, 457–466. [CrossRef]
104. Boehm, A.V.; Meininger, S.; Tesch, A.; Gbureck, U.; Müller, F.A. The mechanical properties of biocompatible apatite bone cement reinforced with chemically activated carbon fibers. *Materials* **2018**, *11*, 192. [CrossRef]
105. Holthaus, M.G.; Stolle, J.; Treccani, L.; Rezwan, K. Orientation of human osteoblasts on hydroxyapatite-based microchannels. *Acta Biomater.* **2012**, *8*, 394–403. [CrossRef]
106. Zhao, C.; Wang, X.; Gao, L.; Jing, L.; Zhou, Q.; Chang, J. The role of the micro-pattern and nano-topography of hydroxyapatite bioceramics on stimulating osteogenic differentiation of mesenchymal stem cells. *Acta Biomater.* **2018**, *73*, 509–521. [CrossRef] [PubMed]
107. Hu, M.; He, Z.; Han, F.; Shi, C.; Zhou, P.; Ling, F.; Zhu, X.; Yang, H.; Li, B. Reinforcement of calcium phosphate cement using alkaline-treated silk fibroin. *Int. J. Nanomed.* **2018**, *13*, 7183–7193. [CrossRef] [PubMed]
108. Ritchie, R.O. The conflicts between strength and toughness. *Nat. Mater.* **2011**, *10*, 817–822. [CrossRef] [PubMed]
109. Zuo, Y.; Yang, F.; Wolke, J.G.C.; Li, Y.; Jansen, J.A. Incorporation of biodegradable electrospun fibers into calcium phosphate cement for bone regeneration. *Acta Biomater.* **2010**, *6*, 1238–1247. [CrossRef] [PubMed]
110. Zan, X.; Sitasuwan, P.; Feng, S.; Wang, Q. Effect of Roughness on in Situ Biomineralized CaP-Collagen Coating on the Osteogenesis of Mesenchymal Stem Cells. *Langmuir* **2016**, *32*, 1808–1817. [CrossRef] [PubMed]

111. Hu, Q.; Tan, Z.; Liu, Y.; Tao, J.; Cai, Y.; Zhang, M.; Pan, H.; Xu, X.; Tang, R. Effect of crystallinity of calcium phosphate nanoparticles on adhesion, proliferation, and differentiation of bone marrow mesenchymal stem cells. *J. Mater. Chem.* **2007**, *17*, 4690–4698. [CrossRef]
112. Mansoorianfar, M.; Shahin, K.; Mirström, M.M.; Li, D. Cellulose-reinforced bioglass composite as flexible bioactive bandage to enhance bone healing. *Ceram. Int.* **2021**, *47*, 416–423. [CrossRef]
113. Dos Santos, L.A.; De Oliveira, L.C.; da Silva Rigo, E.C.; Carrodéguas, R.G.; Boschi, A.O.; Fonseca de Arruda, A.C. Fiber Reinforced Calcium Phosphate Cement. *J. Mech. Behav. Biomed. Mater.* **2000**, *4*, 1658–1671. [CrossRef]
114. Sprio, S.; Ruffini, A.; Dapporto, M.; Tampieri, A. New biomimetic strategies for regeneration of load-bearing bones. In *Bio-Inspired Regenerative Medicine: Materials, Processes and Clinical Applications*; Pan Stanford Publishing: Singapore, 2016; Volume 6, pp. 85–117.
115. Xu, H.H.K.; Eichmiller, F.C.; Giuseppetti, A.A. Reinforcement of a self-setting calcium phosphate cement with different fibers. *J. Biomed. Mater. Res.* **2000**, *52*, 107–114. [CrossRef]
116. Zhang, Y.; Tan, S.; Yin, Y. C-fibre reinforced hydroxyapatite bioceramics. *Ceram. Int.* **2003**, *29*, 113–116. [CrossRef]
117. Li, G.; Zhang, K.; Pei, Z.; Liu, P.; Chang, J.; Zhang, K.; Zhao, S.; Zhang, K.; Jiang, N.; Liang, G. Basalt fibre reinforced calcium phosphate cement with enhanced toughness. *Mater. Technol.* **2020**, *35*, 152–158. [CrossRef]
118. Zhao, X.; Zheng, J.; Zhang, W.; Chen, X.; Gui, Z. Preparation of silicon coated-carbon fiber reinforced HA bio-ceramics for application of load-bearing bone. *Ceram. Int.* **2020**, *46*, 7903–7911. [CrossRef]
119. Dorner-Reisel, A.; Müller, E.; Tomandl, G. Short fiber reinforced hydroxyapatite-based bioceramics. *Adv. Eng. Mater.* **2004**, *6*, 572–577. [CrossRef]
120. Krüger, R.; Groll, J. Fiber reinforced calcium phosphate cements e On the way to degradable load bearing bone substitutes? *Biomaterials* **2012**, *33*, 5887–5900. [CrossRef] [PubMed]
121. Domingues, J.A.; Motisuke, M.; Bertran, C.A.; Hausen, M.A.; De Rezende Duek, E.A.; Camilli, J.A. Addition of Wollastonite Fibers to Calcium Phosphate Cement Increases Cell Viability and Stimulates Differentiation of Osteoblast-Like Cells. *Sci. World J.* **2017**, *2017*, 5260106. [CrossRef] [PubMed]
122. Nezafati, N.; Moztarzadeh, F.; Hesaraki, S.; Mozafari, M. Synergistically reinforcement of a self-setting calcium phosphate cement with bioactive glass fibers. *Ceram. Int.* **2011**, *37*, 927–934. [CrossRef]
123. Petersen, R. Carbon fiber biocompatibility for implants. *Fibers* **2016**, *4*, 1. [CrossRef]
124. Saito, N.; Aoki, K.; Usui, Y.; Shimizu, M.; Hara, K.; Narita, N.; Ogihara, N.; Nakamura, K.; Ishigaki, N.; Kato, H.; et al. Application of carbon fibers to biomaterials: A new era of nano-level control of carbon fibers after 30-years of development. *Chem. Soc. Rev.* **2011**, *40*, 3824–3834. [CrossRef]
125. Siddiqui, H.A.; Pickering, K.L.; Mucalo, M.R. A review on the use of hydroxyapatite- carbonaceous structure composites in bone replacement materials for strengthening purposes. *Materials* **2018**, *11*, 1813. [CrossRef]
126. Motisuke, M.; Santos, V.R.; Bazanini, N.C.; Bertran, C.A. Apatite bone cement reinforced with calcium silicate fibers. *J. Mater. Sci. Mater. Med.* **2014**, *25*, 2357–2363. [CrossRef]
127. Müller, F.A.; Gbureck, U.; Kasuga, T.; Mizutani, Y.; Barralet, J.E.; Lohbauer, U. Whisker-reinforced calcium phosphate cements. *J. Am. Ceram. Soc.* **2007**, *90*, 3694–3697. [CrossRef]
128. Iannotti, V.; Adamiano, A.; Ausanio, G.; Lanotte, L.; Aquilanti, G.; Coey, J.M.D.; Lantieri, M.; Spina, G.; Fittipaldi, M.; Margaris, G.; et al. Fe-Doping-Induced Magnetism in Nano-Hydroxyapatites. *Inorg. Chem.* **2017**, *56*, 4446–4458. [CrossRef] [PubMed]
129. Mastrogiacomo, M.; Corsi, A.; Francioso, E.; Di Comite, M.; Monetti, F.; Scaglione, S.; Favia, A.; Crovace, A.; Bianco, P.; Cancedda, R. Reconstruction of extensive long bone defects in sheep using resorbable bioceramics based on silicon stabilized tricalcium phosphate. *Tissue Eng.* **2006**, *12*, 1261–1273. [CrossRef]
130. Gopi, D.; Shinyjoy, E.; Kavitha, L. Synthesis and spectral characterization of silver/magnesium co-substituted hydroxyapatite for biomedical applications. *Spectrochim. Acta Part A Mol. Biomol. Spectrosc.* **2014**, *127*, 286–291. [CrossRef] [PubMed]
131. Hurle, K.; Oliveira, J.M.; Reis, R.L.; Pina, S.; Goetz-Neunhoeffer, F. Ion-doped Brushite Cements for Bone Regeneration. *Acta Biomater.* **2021**, *123*, 51–71. [CrossRef] [PubMed]
132. Iafisco, M.; Ruffini, A.; Adamiano, A.; Sprio, S.; Tampieri, A. Biomimetic magnesium-carbonate-apatite nanocrystals endowed with strontium ions as anti-osteoporotic trigger. *Mater. Sci. Eng. C* **2014**, *35*, 212–219. [CrossRef] [PubMed]
133. Lim, P.N.; Teo, E.Y.; Ho, B.; Tay, B.Y.; Thian, E.S. Effect of silver content on the antibacterial and bioactive properties of silver-substituted hydroxyapatite. *J. Biomed. Mater. Res. Part A* **2013**, *101 A*, 2456–2464. [CrossRef]
134. Patel, N.; Best, S.M.; Bonfield, W.; Gibson, I.R.; Hing, K.A.; Damien, E.; Revell, P.A. A comparative study on the in vivo behavior of hydroxyapatite and silicon substituted hydroxyapatite granules. *J. Mater. Sci. Mater. Med.* **2002**, *13*, 1199–1206. [CrossRef]
135. Pietak, A.M.; Reid, J.W.; Stott, M.J.; Sayer, M. Silicon substitution in the calcium phosphate bioceramics. *Biomaterials* **2007**, *28*, 4023–4032. [CrossRef]
136. Shi, H.; Zhou, Z.; Li, W.; Fan, Y.; Li, Z.; Wei, J. Hydroxyapatite based materials for bone tissue engineering: A brief and comprehensive introduction. *Crystals* **2021**, *11*, 149. [CrossRef]
137. Gokcekaya, O.; Ueda, K.; Narushima, T.; Ergun, C. Synthesis and characterization of Ag-containing calcium phosphates with various Ca/P ratios. *Mater. Sci. Eng. C* **2015**, *53*, 111–119. [CrossRef] [PubMed]
138. Jadalannagari, S.; Deshmukh, K.; Ramanan, S.R.; Kowshik, M. Antimicrobial activity of hemocompatible silver doped hydroxyapatite nanoparticles synthesized by modified sol–gel technique. *Appl. Nanosci.* **2014**, *4*, 133–141. [CrossRef]

139. Sprio, S.; Preti, L.; Montesi, M.; Panseri, S.; Adamiano, A.; Vandini, A.; Pugno, N.M.; Tampieri, A. Surface Phenomena Enhancing the Antibacterial and Osteogenic Ability of Nanocrystalline Hydroxyapatite, Activated by Multiple-Ion Doping. *ACS Biomater. Sci. Eng.* **2019**, *5*, 5947–5959. [CrossRef] [PubMed]
140. Stanić, V.; Janaćković, D.; Dimitrijević, S.; Tanasković, S.B.; Mitrić, M.; Pavlović, M.S.; Krstić, A.; Jovanović, D.; Raičević, S. Synthesis of antimicrobial monophase silver-doped hydroxyapatite nanopowders for bone tissue engineering. *Appl. Surf. Science* **2011**, *257*, 4510–4518. [CrossRef]
141. Pors Nielsen, S. The biological role of strontium. *Bone* **2004**, *35*, 583–588. [CrossRef]
142. Ge, X.; Leng, Y.; Bao, C.; Xu, S.L.; Wang, R.; Ren, F. Antibacterial coatings of fluoridated hydroxyapatite for percutaneous implants. *J. Biomed. Mater. Res. Part A* **2010**, *95 A*, 588–599. [CrossRef]
143. Pina, S.; Torres, P.M.; Goetz-Neunhoeffer, F.; Neubauer, J.; Ferreira, J.M.F. Newly developed Sr-substituted α-TCP bone cements. *Acta Biomater.* **2010**, *6*, 928–935. [CrossRef]
144. Wang, L.; He, S.; Wu, X.; Liang, S.; Mu, Z.; Wei, J.; Deng, F.; Deng, Y.; Wei, S. Polyetheretherketone/nano-fluorohydroxyapatite composite with antimicrobial activity and osseointegration properties. *Biomaterials* **2014**, *35*, 6758–6775. [CrossRef]
145. Tampieri, A.; D'Alessandro, T.; Sandri, M.; Sprio, S.; Landi, E.; Bertinetti, L.; Panseri, S.; Pepponi, G.; Goettlicher, J.; Bañobre-López, M.; et al. Intrinsic magnetism and hyperthermia in bioactive Fe-doped hydroxyapatite. *Acta Biomater.* **2012**, *8*, 843–851. [CrossRef]
146. Degli Esposti, L.; Markovic, S.; Ignjatovic, N. Thermal crystallization of amorphous calcium phosphate combined with citrate and fluoride doping: A novel route to produce hydroxyapatite bioceramics. *J. Mater. Chem. B* **2021**, *10*. [CrossRef]
147. Yin, X.; Bai, Y.; Zhou, S.j.; Ma, W.; Bai, X.; Chen, W.d. Solubility, Mechanical and Biological Properties of Fluoridated Hydroxyapatite/Calcium Silicate Gradient Coatings for Orthopedic and Dental Applications. *J. Therm. Spray Technol.* **2020**, *29*, 471–488. [CrossRef]
148. He, W.; Zhou, Y.T.; Wamer, W.G.; Boudreau, M.D.; Yin, J.J. Mechanisms of the pH dependent generation of hydroxyl radicals and oxygen induced by Ag nanoparticles. *Biomaterials* **2012**, *33*, 7547–7555. [CrossRef]
149. Klammert, U.; Ignatius, A.; Wolfram, U.; Reuther, T.; Gbureck, U. In vivo degradation of low temperature calcium and magnesium phosphate ceramics in a heterotopic model. *Acta Biomater.* **2011**, *7*, 3469–3475. [CrossRef] [PubMed]
150. Cao, X.; Harris, W. Carbonate and magnesium interactive effect on calcium phosphate precipitation. *Environ. Sci. Technol.* **2008**, *42*, 436–442. [CrossRef]
151. Salimi, M.H.; Heughebaert, J.C.; Nancollas, G.H. Crystal Growth of Calcium Phosphates in the Presence of Magnesium Ions. *Langmuir* **1985**, *1*, 119–122. [CrossRef]
152. Wang, L.; Nancollas, G.H. Calcium orthophosphates: Crystallization and Dissolution. *Chem. Rev.* **2008**, *108*, 4628–4669. [CrossRef]
153. Cao, X.; Harris, W.G.; Josan, M.S.; Nair, V.D. Inhibition of calcium phosphate precipitation under environmentally-relevant conditions. *Sci. Total Environ.* **2007**, *383*, 205–215. [CrossRef] [PubMed]
154. Diallo-Garcia, S.; Laurencin, D.; Krafft, J.M.; Casale, S.; Smith, M.E.; Lauron-Pernot, H.; Costentin, G. Influence of magnesium substitution on the basic properties of hydroxyapatites. *J. Phys. Chem. C* **2011**, *115*, 24317–24327. [CrossRef]
155. Bianchi, M.; Degli Esposti, L.; Ballardini, A.; Liscio, F.; Berni, M.; Gambardella, A.; Leeuwenburgh, S.C.G.; Sprio, S.; Tampieri, A.; Iafisco, M. Strontium doped calcium phosphate coatings on poly(etheretherketone) (PEEK) by pulsed electron deposition. *Surf. Coat. Technol.* **2017**, *319*, 191–199. [CrossRef]
156. Guo, D.; Xu, K.; Zhao, X.; Han, Y. Development of a strontium-containing hydroxyapatite bone cement. *Biomaterials* **2005**, *26*, 4073–4083. [CrossRef]
157. Marie, P.J. Strontium as therapy for osteoporosis. *Curr. Opin. Pharmacol.* **2005**, *5*, 633–636. [CrossRef]
158. Montesi, M.; Panseri, S.; Dapporto, M.; Tampieri, A.; Sprio, S. Sr-substituted bone cements direct mesenchymal stem cells, osteoblasts and osteoclasts fate. *PLoS ONE* **2017**, *12*, e0172100. [CrossRef]
159. Sprio, S.; Dapporto, M.; Montesi, M.; Panseri, S.; Lattanzi, W.; Pola, E.; Logroscino, G.; Tampieri, A. Novel Osteointegrative Sr-Substituted Apatitic Cements Enriched with Alginate. *Materials* **2016**, *9*, 763. [CrossRef]
160. Landi, E.; Tampieri, A.; Celotti, G.; Sprio, S.; Sandri, M.; Logroscino, G. Sr-substituted hydroxyapatites for osteoporotic bone replacement. *Acta Biomater.* **2007**, *3*, 961–969. [CrossRef]
161. Biris, A.R.; Mahmood, M.; Lazar, M.D.; Dervishi, E.; Watanabe, F.; Mustafa, T.; Baciut, G.; Baciut, M.; Bran, S.; Ali, S.; et al. Novel multicomponent and biocompatible nanocomposite materials based on few-layer graphenes synthesized on a gold/hydroxyapatite catalytic system with applications in bone regeneration. *J. Phys. Chem. C* **2011**, *115*, 18967–18976. [CrossRef]
162. Liang, W.; Gao, M.; Lou, J.; Bai, Y.; Zhang, J.; Lu, T.; Sun, X.; Ye, J.; Li, B.; Sun, L.; et al. Integrating silicon/zinc dual elements with PLGA microspheres in calcium phosphate cement scaffolds synergistically enhances bone regeneration. *J. Mater. Chem. B* **2020**. [CrossRef] [PubMed]
163. Zhu, J.; Wong, H.M.; Yeung, K.W.K.; Tjong, S.C. Spark plasma sintered hydroxyapatite/graphite nanosheet and hydroxyapatite/multiwalled carbon nanotube composites: Mechanical and in vitro cellular properties. *Adv. Eng. Mater.* **2011**, *13*, 336–341. [CrossRef]
164. Dong, G.; Zheng, Y.; He, L.; Wu, G.; Deng, C. The effect of silicon doping on the transformation of amorphous calcium phosphate to silicon-substituted α-tricalcium phosphate by heat treatment. *Ceram. Int.* **2016**, *42*, 883–890. [CrossRef]

165. Mestres, G.; Le Van, C.; Ginebra, M.P. Silicon-stabilized α-tricalcium phosphate and its use in a calcium phosphate cement: Characterization and cell response. *Acta Biomater.* **2012**, *8*, 1169–1179. [CrossRef] [PubMed]
166. Feng, Q.; Liu, Y.; Huang, J.; Chen, K.; Huang, J.; Xiao, K. Uptake, distribution, clearance, and toxicity of iron oxide nanoparticles with different sizes and coatings. *Sci. Rep.* **2018**, *8*, 2082. [CrossRef]
167. Manchón, A.; Hamdan Alkhraisat, M.; Rueda-Rodriguez, C.; Prados-Frutos, J.C.; Torres, J.; Lucas-Aparicio, J.; Ewald, A.; Gbureck, U.; López-Cabarcos, E. A new iron calcium phosphate material to improve the osteoconductive properties of a biodegradable ceramic: A study in rabbit calvaria. *Biomed. Mater.* **2015**, *10*, 055012. [CrossRef] [PubMed]
168. Perez, R.A.; Patel, K.D.; Kim, H.W. Novel magnetic nanocomposite injectables: Calcium phosphate cements impregnated with ultrafine magnetic nanoparticles for bone regeneration. *RSC Adv.* **2015**, *5*, 13411–13419. [CrossRef]
169. Xu, C.; Zheng, Y.; Gao, W.; Xu, J.; Zuo, G.; Chen, Y.; Zhao, M.; Li, J.; Song, J.; Zhang, N.; et al. Magnetic Hyperthermia Ablation of Tumors Using Injectable Fe3O4/Calcium Phosphate Cement. *ACS Appl. Mater. Interfaces* **2015**, *7*, 13866–13875. [CrossRef]
170. Panseri, S.; Cunha, C.; D'Alessandro, T.; Sandri, M.; Giavaresi, G.; Marcacci, M.; Hung, C.T.; Tampieri, A. Intrinsically superparamagnetic Fe-hydroxyapatite nanoparticles positively influence osteoblast-like cell behaviour. *J. Nanobiotechnol.* **2012**, *10*, 1. [CrossRef]
171. Degli Esposti, L.; Adamiano, A.; Tampieri, A.; Ramirez-Rodriguez, G.B.; Siliqi, D.; Giannini, C.; Ivanchenko, P.; Martra, G.; Lin, F.H.; Delgado-López, J.M.; et al. Combined Effect of Citrate and Fluoride Ions on Hydroxyapatite Nanoparticles. *Cryst. Growth Des.* **2020**, *20*, 3163–3172. [CrossRef]
172. Guo, H.; Wei, J.; Yuan, Y.; Liu, C. Development of calcium silicate/calcium phosphate cement for bone regeneration. *Biomed. Mater.* **2007**, *2*, S153–S159. [CrossRef]
173. Sprio, S.; Tampieri, A.; Celotti, G.; Landi, E. Development of hydroxyapatite/calcium silicate composites addressed to the design of load-bearing bone scaffolds. *J. Mech. Behav. Biomed. Mater.* **2009**, *2*, 147–155. [CrossRef] [PubMed]
174. Hesaraki, S.; Alizadeh, M.; Borhan, S.; Pourbaghi-Masouleh, M. Polymerizable nanoparticulate silica-reinforced calcium phosphate bone cement. *J. Biomed. Mater. Res. Part B Appl. Biomater.* **2012**, *100 B*, 1627–1635. [CrossRef]
175. Mohammadi, M.; Hesaraki, S.; Hafezi-Ardakani, M. Investigation of biocompatible nanosized materials for development of strong calcium phosphate bone cement: Comparison of nano-titania, nano-silicon carbide and amorphous nano-silica. *Ceram. Int.* **2014**, *40*, 8377–8387. [CrossRef]
176. Golzar, H.; Mohammadrezaei, D.; Yadegari, A.; Rasoulianboroujeni, M.; Hashemi, M.; Omidi, M.; Yazdian, F.; Shalbaf, M.; Tayebi, L. Incorporation of functionalized reduced graphene oxide/magnesium nanohybrid to enhance the osteoinductivity capability of 3D printed calcium phosphate-based scaffolds. *Compos. Part B Eng.* **2020**, *185*, 107749. [CrossRef]
177. Shi, Y.Y.; Li, M.; Liu, Q.; Jia, Z.J.; Xu, X.C.; Cheng, Y.; Zheng, Y.F. Electrophoretic deposition of graphene oxide reinforced chitosan–hydroxyapatite nanocomposite coatings on Ti substrate. *J. Mater. Sci. Mater. Med.* **2016**, *27*, 1–13. [CrossRef] [PubMed]
178. Wang, S.; Zhang, S.; Wang, Y.; Sun, X.; Sun, K. Reduced graphene oxide/carbon nanotubes reinforced calcium phosphate cement. *Ceram. Int.* **2017**, *43*, 13083–13088. [CrossRef]
179. Medvecky, L.; Stulajterova, R.; Giretova, M.; Sopcak, T.; Faberova, M. Properties of CaO-SiO_2-P_2O_5 reinforced calcium phosphate cements and in vitro osteoblast response. *Biomed. Mater.* **2017**, *12*, aa5b3b. [CrossRef]
180. Yu, L.; Li, Y.; Zhao, K.; Tang, Y.; Cheng, Z.; Chen, J.; Zang, Y.; Wu, J.; Kong, L.; Liu, S.; et al. A Novel Injectable Calcium Phosphate Cement-Bioactive Glass Composite for Bone Regeneration. *PLoS ONE* **2013**, *8*, e62570. [CrossRef] [PubMed]
181. Aparicio, J.L.; Rueda, C.; Manchón, Á.; Ewald, A.; Gbureck, U.; Alkhraisat, M.H.; Jerez, L.B.; Cabarcos, E.L. Effect of physicochemical properties of a cement based on silicocarnotite/calcium silicate on in vitro cell adhesion and in vivo cement degradation. *Biomed. Mater.* **2016**, *11*, 045005. [CrossRef]
182. Sopcak, T.; Medvecky, L.; Giretova, M.; Stulajterova, R.; Molcanova, Z.; Podobova, M.; Girman, V. Physical, mechanical and in vitro evaluation of a novel cement based on akermantite and dicalcium phosphate dihydrate phase. *Biomed. Mater.* **2019**, *14*, ab216d. [CrossRef]
183. Kapat, K.; Shubhra, Q.T.H.; Zhou, M.; Leeuwenburgh, S. Piezoelectric Nano-Biomaterials for Biomedicine and Tissue Regeneration. *Adv. Funct. Mater.* **2020**, *30*, 201909045. [CrossRef]
184. Polley, C.; Distler, T.; Detsch, R.; Lund, H.; Springer, A.; Boccaccini, A.R.; Seitz, H. 3D printing of piezoelectric barium titanate-hydroxyapatite scaffolds with interconnected porosity for bone tissue engineering. *Materials* **2020**, *13*, 1773. [CrossRef]
185. Li, M.; Xiong, P.; Yan, F.; Li, S.; Ren, C.; Yin, Z.; Li, A.; Li, H.; Ji, X.; Zheng, Y.; et al. An overview of graphene-based hydroxyapatite composites for orthopedic applications. *Bioact. Mater.* **2018**, *3*, 1–18. [CrossRef]
186. Tanaka, M.; Aoki, K.; Haniu, H.; Kamanaka, T.; Takizawa, T.; Sobajima, A.; Yoshida, K.; Okamoto, M.; Kato, H.; Saito, N. Applications of carbon nanotubes in bone regenerative medicine. *Nanomaterials* **2020**, *10*, 659. [CrossRef] [PubMed]
187. Zhang, Y.; Nayak, T.R.; Hong, H.; Cai, W. Graphene: A versatile nanoplatform for biomedical applications. *Nanoscale* **2012**, *4*, 3833–3842. [CrossRef] [PubMed]
188. Barabás, R.; de Souza Ávila, E.; Ladeira, L.O.; Antônio, L.M.; Tötös, R.; Simedru, D.; Bizo, L.; Cadar, O. Graphene Oxides/Carbon Nanotubes–Hydroxyapatite Nanocomposites for Biomedical Applications. *Arab. J. Sci. Eng.* **2020**, *45*, 219–227. [CrossRef]
189. Gonçalves, E.M.; Oliveira, F.J.; Silva, R.F.; Neto, M.A.; Fernandes, M.H.; Amaral, M.; Vallet-Regí, M.; Vila, M. Three-dimensional printed PCL-hydroxyapatite scaffolds filled with CNTs for bone cell growth stimulation. *J. Biomed. Mater. Res. Part B Appl. Biomater.* **2016**, *104*, 1210–1219. [CrossRef] [PubMed]

190. Han, Y.H.; Gao, R.; Bajpai, I.; Kim, B.N.; Yoshida, H.; Nieto, A.; Son, H.W.; Yun, J.; Jang, B.K.; Jhung, S.; et al. Spark plasma sintered bioceramics–from transparent hydroxyapatite to graphene nanocomposites: A review. *Adv. Appl. Ceram.* **2020**, *119*, 57–74. [CrossRef]
191. Jakus, A.E.; Shah, R.N. Multi and mixed 3D-printing of graphene-hydroxyapatite hybrid materials for complex tissue engineering. *J. Biomed. Mater. Res. Part A* **2017**, *105*, 274–283. [CrossRef]
192. Liu, Y.; Dang, Z.; Wang, Y.; Huang, J.; Li, H. Hydroxyapatite/graphene-nanosheet composite coatings deposited by vacuum cold spraying for biomedical applications: Inherited nanostructures and enhanced properties. *Carbon* **2014**, *67*, 250–259. [CrossRef]
193. Mata, D.; Oliveira, F.J.; Neto, M.A.; Belmonte, M.; Bastos, A.C.; Lopes, M.A.; Gomes, P.S.; Fernandes, M.H.; Silva, R.F. Smart electroconductive bioactive ceramics to promote in situ electrostimulation of bone. *J. Mater. Chem. B* **2015**, *3*, 1831–1845. [CrossRef]
194. Zhang, L.; Liu, W.; Yue, C.; Zhang, T.; Li, P.; Xing, Z.; Chen, Y. A tough graphene nanosheet/hydroxyapatite composite with improved in vitro biocompatibility. *Carbon* **2013**, *61*, 105–115. [CrossRef]
195. Wang, S.; Sun, X.; Wang, Y.; Sun, K.; Bi, J. Properties of reduced graphene/carbon nanotubes reinforced calcium phosphate bone cement in a microwave environment. *J. Mater. Sci. Mater. Med.* **2019**, *30*, 37. [CrossRef]
196. Dapporto, M.; Tampieri, A.; Sprio, S. Composite Calcium Phosphate/Titania Scaffolds in Bone Tissue Engineering. In *Application of Titanium Dioxide*; InTechOpen: London, UK, 2017.
197. Roguska, A.; Pisarek, M.; Andrzejczuk, M.; Dolata, M.; Lewandowska, M.; Janik-Czachor, M. Characterization of a calcium phosphate-TiO2 nanotube composite layer for biomedical applications. *Mater. Sci. Eng. C* **2011**, *31*, 906–914. [CrossRef]
198. Cunha, C.; Sprio, S.; Panseri, S.; Dapporto, M.; Marcacci, M.; Tampieri, A. High biocompatibility and improved osteogenic potential of novel Ca-P/titania composite scaffolds designed for regeneration of load-bearing segmental bone defects. *J. Biomed. Mater. Res. Part A* **2013**, *101 A*, 1612–1619. [CrossRef]
199. Sprio, S.; Guicciardi, S.; Dapporto, M.; Melandri, C.; Tampieri, A. Synthesis and mechanical behavior of β-tricalcium phosphate/titania composites addressed to regeneration of long bone segments. *J. Mech. Behav. Biomed. Mater. 2013 17*, 1–10. [CrossRef]
200. Liu, H.; Guan, Y.; Wei, D.; Gao, C.; Yang, H.; Yang, L. Reinforcement of injectable calcium phosphate cement by gelatinized starches. *J. Biomed. Mater. Res. Part B Appl. Biomater.* **2016**, *104*, 615–625. [CrossRef] [PubMed]
201. Tandon, B.; Blaker, J.J.; Cartmell, S.H. Piezoelectric materials as stimulatory biomedical materials and scaffolds for bone repair. *Acta Biomater.* **2018**, *73*, 1–20. [CrossRef] [PubMed]